OUKA
The University of Osaka
Institutional Knowledge Archive

Title	Biochemical Analysis of Photoreceptor Ca2+-Binding Proteins
Author(s)	松田, 信爾
Citation	大阪大学, 1998, 博士論文
Version Type	VoR
URL	https://doi.org/10.11501/3143769
rights	
Note	

The University of Osaka Institutional Knowledge Archive : OUKA

https://ir.library.osaka-u.ac.jp/

The University of Osaka

１９９７年度

博士論文

Biochemical Analysis of Photoreceptor Ca^{2+}-Binding Proteins

（視細胞特異的Ca^{2+}結合タンパク質の生物化学的研究）

大阪大学　大学院理学研究科　生物化学専攻

松田信爾

CONTENTS

要旨（Abstract）

はじめに

暗条件下での脊椎動物の視細胞においては、cGMP依存性陽イオンチャンネルが開いており、陽イオンが細胞内へ流入している。流入する陽イオンの大部分はNa^+であるがCa^{2+}も同時に流入している。細胞内へ流入したCa^{2+}はNa^+-K^+/Ca^{2+}交換機構により細胞外へ排出されている。視物質が光を受けると、Gタンパク質、ホスホジエステラーゼが順次活性化され、cGMP依存性陽イオンチャンネルが閉じる。それに伴い、細胞内への陽イオンの流入が止まり、視細胞が過分極する。Na^+-K^+/Ca^{2+}交換機構は光とは無関係に、Ca^{2+}を排出し続けるので、明条件下では、暗条件下に比べ視細胞内Ca^{2+}濃度は減少する。このCa^{2+}濃度の変化が、視細胞の順応に重要であることが明らかにされてきた。カエル視細胞には高Ca^{2+}濃度でロドプシンのリン酸化を阻害するタンパク質（Ｓ－モジュリン）が存在している。ロドプシンのリン酸化はロドプシンの不活性化に重要であるので、Ｓ－モジュリンは高Ca^{2+}濃度で活性型ロドプシンの寿命を引き延ばし、順応に関与していると考えられる。近年、中枢神経系においても、Ｓ－モジュリン類似タンパク質の存在が明らかにされてきており、Ｓ－モジュリンの研究がこれらの研究の先駆的な役割を果たすものと期待できる。

錐体型Ｓ－モジュリン（ｓ２６）のクローン化

私は、カエル網膜中の新たなCa^{2+}結合タンパク質（ｓ２６）をクローン化した。推定されるｓ２６のアミノ酸配列は、ビジニン（ニワトリ網膜に存在すると考えられているタンパク質）のものと７７％、Ｓ－モジュリンのものと６７％が一致していた。免疫組織化学的手法を用いてＳ－モジュリン、ｓ２６のカエル網膜中での局在を調べたところ、Ｓ－モジュリンは桿体視細胞に、ｓ２６は錐体視細胞に存在することが明らかになった。このことから脊椎動物のＳ－モジュリン類似タンパク質には桿体型と錐体型の少なくとも２種類のサブタイプが存在していることが明らかになった。

Ｓ－モジュリン、ｓ２６の発現

Ｓ－モジュリン、ｓ２６のＮ末にはミリストイル基付加シグナルがあり、脂肪酸修飾されていると考えられる。以下の方法により、Ｎ末未修飾のＳ－モジュリンとｓ２６、及びＮ末ミリストイル化したＳ－モジュリンとｓ２６の４種をそれぞれ大腸菌の系で発現させ、１ℓの培養液から数十mgのタンパク質を精製することに成功した。Ｓ－モジュリン、ｓ２６をコードするDNA断片を発現ベクター（pET-16b）に組み込み、大腸菌（BL21DE3）を形質転換し、IPTGを加えて発現を誘導した。Ｎ末のミリストイル化はミリストイルトランスフェラーゼを共発現させ、培養液にミリスチン酸を加えることにより行った。発現したタンパク質は封入体として存在したため、尿素で可溶化した後、再構成させた。これらのタンパク質は天然のＳ－モジュリン、ｓ２６と同様の方法で精製可能であった。

N末ミリストイル化S－モジュリン、及びs２６のCa^{2+}濃度に依存したトリプトファンの蛍光スペクトル変化を比較したところ、両者のCa^{2+}結合定数に大きな差は見られなかった。また、N末ミリストイル化タンパク質は高Ca^{2+}濃度で視細胞外節膜に結合したが、未修飾のタンパク質はわずかしか結合しなかった。このことから、N末のミリストイル化は視細胞外節膜への結合に重要であることが示された。

S－モジュリンのC末付近の電荷の役割

視細胞外節膜に対する結合性を調べたところ、S－モジュリンはs２６に比べて、より強い結合性を持っていることが明らかになった。N末から１７３番目のアミノ酸までがs２６の配列、C末の２９アミノ酸がS－モジュリンの配列を持ったキメラs２６はS－モジュリンと同等の膜結合性を示した。これに対し、逆の組み合わせのキメラS－モジュリンはs２６と同等の膜結合性を示した。またC末付近の正電荷を除去した変異S－モジュリンはs２６以下の結合性しか示さなかったが、負電荷を除去したS－モジュリンでは、野生型のS－モジュリン以上の膜結合性を示した。また、これらのタンパク質のロドプシンのリン酸化に対する影響を調べた結果、高い膜結合性を持つタンパク質は膜結合性の低いタンパク質に比べ、より効率的にロドプシンのリン酸化を阻害した。このことからS－モジュリンのC末の正電荷は、膜への結合性を高め、それによりロドプシンのリン酸化阻害効率を高めていると考えられる。視細胞に存在するS－モジュリン類似タンパク質は桿体型と錐体型に分けられるが、桿体型は錐体型に比べC末付近により多くの正電荷を持つアミノ酸を含んでいる。このためより強く視細胞外節膜に結合し、より効率よく、ロドプシンのリン酸化を阻害すると考えられる。錐体は桿体に比べて、より早く光応答が終結することが知られている。s２６がS－モジュリンに比べて視物質リン酸化阻害の効率が低いことが錐体の早い光応答終結に関与している可能性が考えられる。

S－モジュリンのそれぞれのカルシウム結合部位の役割

S－モジュリンには4つのEF-handモチーフが存在するが、そのうちCa^{2+}を結合できるのはEF-hand 2とEF-hand 3の２ヶ所である。このうちの一方を部位特異的変異によって不活化することで、それぞれのEF-handが担う役割を調べた。EF-hand 2を不活化した変異体（E85M)とEF-hand 3を不活化した変異体（E121M)のCa^{2+}非結合状態でのトリプトファンの蛍光スペクトルは野生型S－モジュリンのものとほぼ一致した。このことから変異の導入はS－モジュリンの構造を大きく破壊していないと考えられる。予想されるように、野生型S－モジュリンは１分子当たり２つのCa^{2+}を結合し、E85Mは１分子当たり１つのCa^{2+}を結合した。これに対して、E121M はCa^{2+}を結合しなかった。このことから、EF-hand 3へのCa^{2+}の結合がEF-hand 2へのCa^{2+}の結合に重要であると考えられる。E85Mは野生型S－モジュリンと同等に視細胞外節膜に結合するが、ロドプシンのリン酸化は阻害しなかった。このことから、EF-hand 3へのCa^{2+}の結合はS－モジュリンの視細胞外節膜への結合を引き起こし、EF-hand 2へのCa^{2+}の結合がロドプシンのリン酸化の阻害に必要であることが示唆された。

Chapter 1

Introduction

Photoreceptor is a highly specialized neuron which responds to light and transmits electrical signals to secondary neurons. Rod photoreceptors of vertebrates are one of the most well-studied neurons by using physiological and biochemical techniques. In the dark adapted vertebrate rod photoreceptor cell, cGMP-gated cation channels are opened and a steady current flows into the cell (1, 2). Most of this current (~70%) is carried by Na^+, but a small portion (~15%) is carried by Ca^{2+} (3). This Ca^{2+} entered into the cell is continuously pumped out by a Na^+-K^+, Ca^{2+} exchanger (4, 5). Light activates visual pigments, which activates GTP-binding proteins (transducin) (Fig. 1-1). Then the activated transducin activates phosphodiesterases (PDE), which cause the decreasement of the cytoplasmic cGMP concentration. Consequently, cGMP gated cation channels are closed, and the photoreceptor is hyperpolarized. Since the entry of Ca^{2+} is blocked, during light-adaptation, the cytoplasmic Ca^{2+} concentration is decreased. This change of the cytoplasmic Ca^{2+} concentration is the underlying mechanism of the photoreceptor's adaptation (6, 7).

The phosphorylation by rhodopsin kinase is important for the deactivation of light-activated rhodopsin (8, 9). A Ca^{2+}-binding protein (S-modulin) found in frog rods inhibits the rhodopsin kinase activity at high Ca^{2+} concentrations, but does not interfere at low Ca^{2+} concentrations (Fig. 1-2) (10). In this mechanism, S-modulin contributes to increase the light-sensitivity of the dark-adapted rod photoreceptor cell. Since S-modulin is one of the key proteins in the adaptation, great efforts were made by many groups to clarify the molecular mechanism of S-modulin. For example, Ames *et al* investigated the structures of Ca^{2+}-free and Ca^{2+}-binding forms of S-modulin by NMR technique (Fig. 1-3) (11). Zozulya *et al* and Dizhoor *et al* indicated that the N-terminus of S-modulin is myristoylated, and the Ca^{2+}-binding causes the exposure of myristoyl group, which enables S-modulin to bind ROS membrane (12, 13). This property is called " Ca^{2+}-myristoyl switch" and may be important for S-modulin functions. Recently

S-modulin like proteins were found in the central nerve systems, so the knowledge of S-modulin may lead us to understand the modulation system of these neurons.

There are two kinds of photoreceptor cells, rods and cones which are thought to be responsible for the twilight and daylight vision, respectively. Rods are more sensitive than cones, and the light response of cones is faster and is terminated more rapidly than that of rods (14) (Fig. 1-4). Recent works suggest that the signal transduction pathway of cones is similar to that of rods, and there are rod and cone types of proteins participating in the phototransduction (15-19).

In the chapter 2, cDNA encoding s26 (a Ca^{2+}-binding protein in frog retina) was isolated, and the localization of S-modulin and s26 was investigated. It was shown that s26 is a cone homologue of S-modulin. The difference in the amino acid sequence between S-modulin and s26 is found mainly in carboxyl terminal regions. That is S-modulin C-terminus has more charged amino acids than that of s26. In the chapter 3, the over-expression system of S-modulin and s26 were established, and biochemical properties were investigated. In the chapter 4, the role of carboxyl terminal charges of S-modulin were investigated by using chimeric and site directed-mutants. It was indicated that the C-terminal positive charge of S-modulin enhances rod outer segment (ROS) membrane association and increased the inhibitory efficiency on rhodopsin phosphorylation.

There are four EF-hand motifs in S-modulin, but only two of them (EF-hand 2 and 3) are thought to be able to bind Ca^{2+} (20). Therefore, Ca^{2+}-binding to these regions induce ROS membrane-association and inhibition of rhodopsin phosphorylation. In the chapter 5, the role of each EF-hand was investigated by using site directed mutants. It was suggested that Ca^{2+}-binding to EF-3 induces the exposure of myristoyl group, and enables EF-2 to be a functional Ca^{2+}-binding site. Ca^{2+}-binding to EF-2 is essential for the inhibition of rhodopsin phosphorylation.

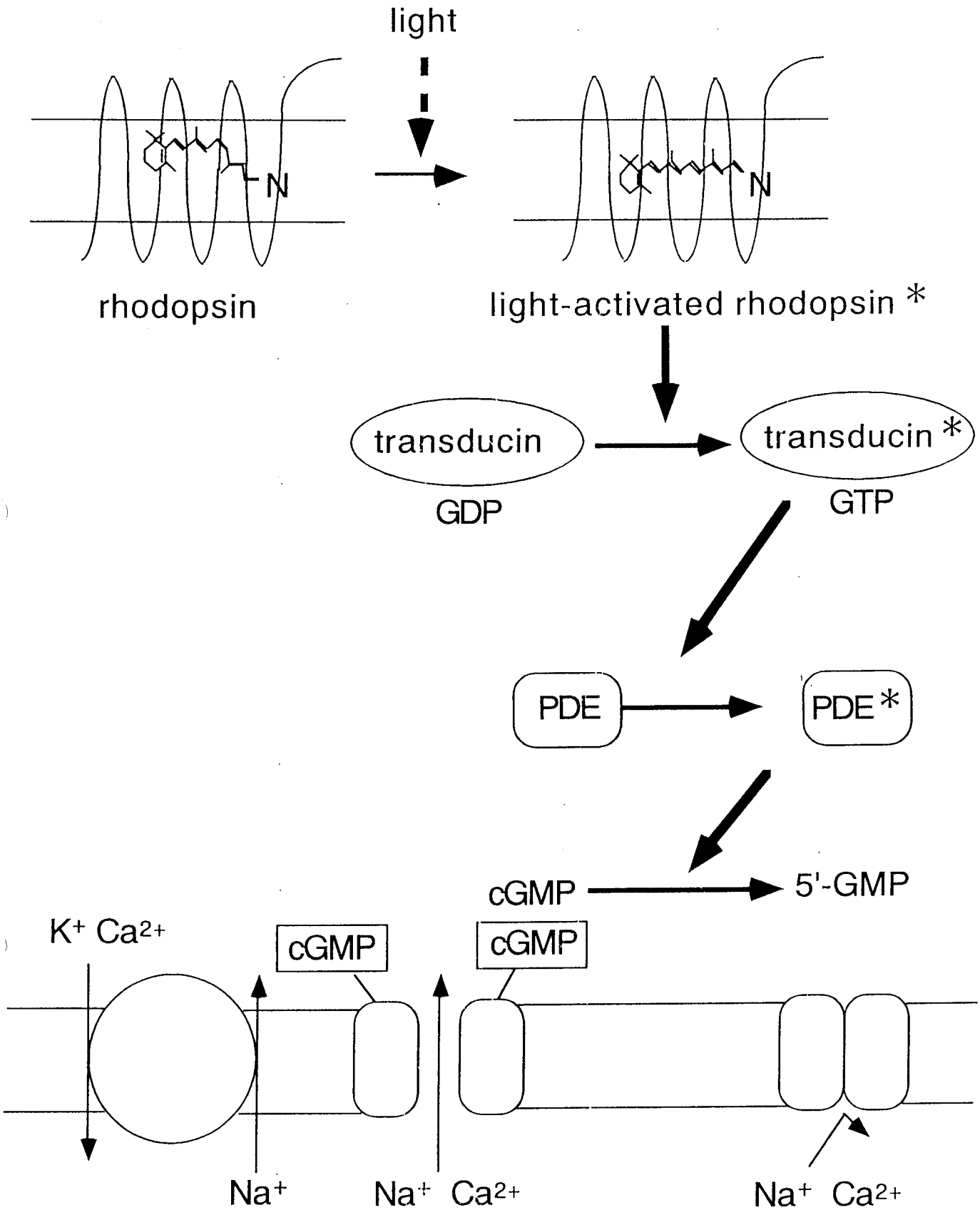

Figure1-1: A scheme of photo transduction cascade. * indicates activated sates.

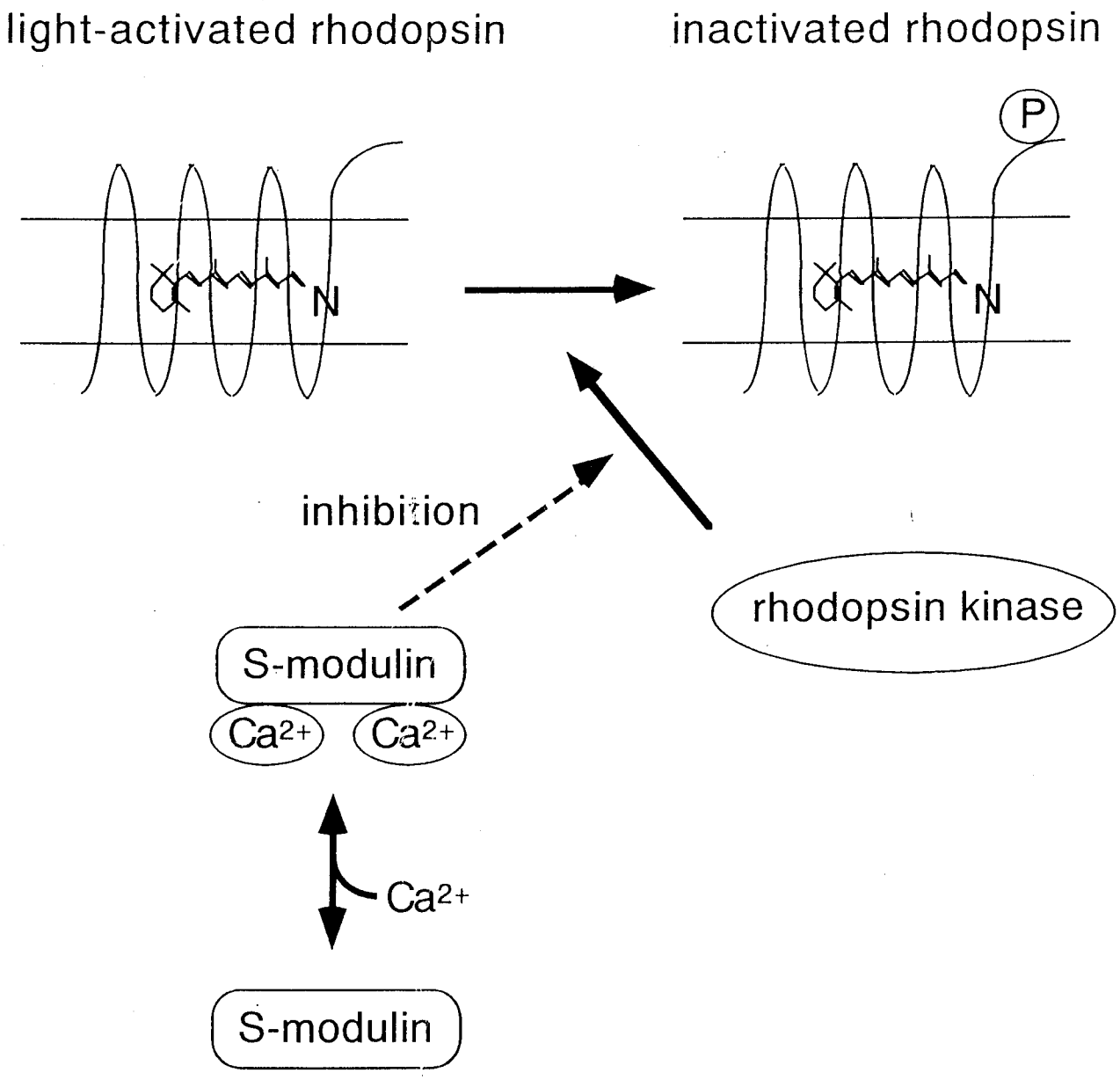

Figure 1-2: Inhibition of rhodopsin phosphorylation by S-modulin

A

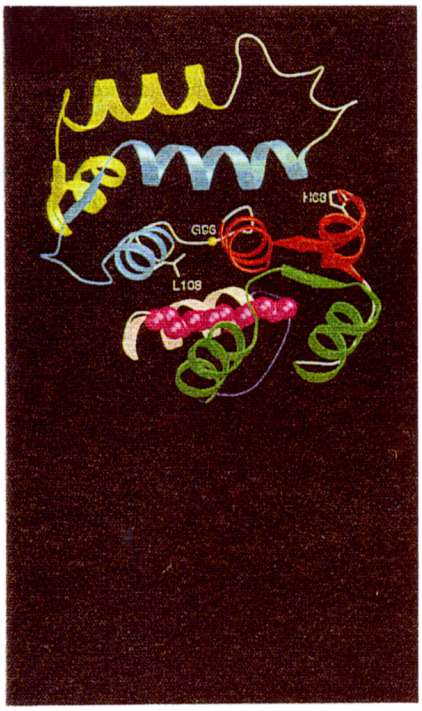

B

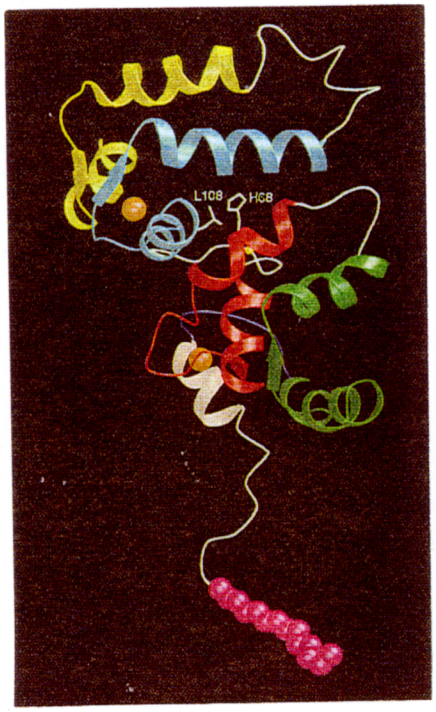

Figure 1-3: Three dimensional structures of bovine S-modulin (recoverin) determined by NMR (11). A and B indicate the Ca^{2+}-free and Ca^{2+}-bound forms, respectively.

A

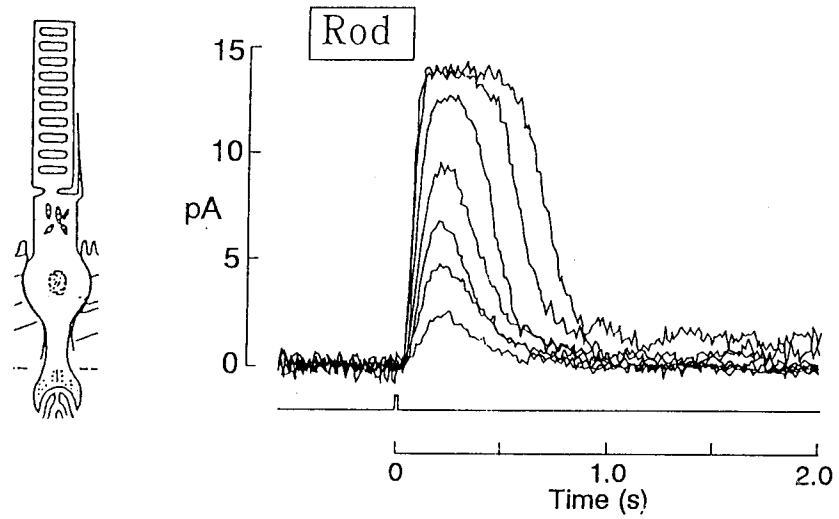

B

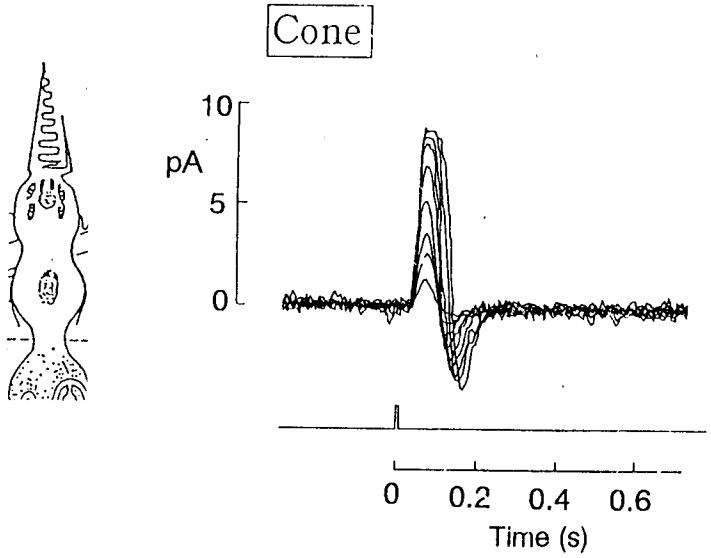

Figure 1-4: A and B indicate the photo-response of rod and cone photoreceptor cells, respectively (21, 22).

References

1. Stryer, L. (1986) Annu. Rev. Neurosci. 9, 87-119

2. Kaupp. U. B., and Koch, K.-W. (1992) Annu. Rev. Physiol. 54, 153-175

3. Nakatani, K., and Yau, K.-W. (1988) J. Physiol. (London) 395, 695-729

4. Yau, K.-W., and Nakatani, K. (1985) Nature 313, 579-582

5. McNaughton, P. A., Cervetto, L., and Nunn, B. J. (1986) Nature 322, 261-263

6. Matthews, H. R., Murphy, R. L. W., Fain, G., and Lam, T. D. (1988) Nature 334, 67-69

7. Nakatani, K., and Yau, K.-W. (1988) Nature 334, 69-71

8. Palczewski, K., Buczylko, J., Lebioda, L., Crabb, J. W., and Polans, A. S. (1993) J. Biol. Chem. 268, 14579-14582

9. Chen, J., Makino, C. L., Peachey, N. S., Baylor, D. A., and Simon, M. I. (1995) Science 267, 374-376

10. Kawamura, S. (1993) Nature 362, 855-847

11. Ames, J. B., Ishima, R., Toshiyuki, T., Gordon, J. I., Stryer, L., and Ikura, M. (1997) Nature 389, 198-202

12. Zozulya, S., and Stryer, L. (1992) Proc. Natl. Acad. Sci. U. S. A. 89, 11569-11573

13. Dizhoor, A. M., Chen, C. K., Olshevskaya, E., Sinelnikova, V. V., Phillipov, P., and Hurley, J. B. (1993) Science 259, 829-832

14. Cobbs, W. H., Barkdoll, A. E., and Pugh, E. N. (1985) Nature 317, 64-66

15. Nathans, J., Thomas, D., and Hogness, D. S. (1986) Science 232, 193-202

16. Lerea, C. L., Somers, D. E., Hurley, J. B., Klock, I. B., and Bunt-Milam, A. H. (1986) Science 234, 77-80

17. Baylor, D. A. (1987) Invest. Opthalmol. Visual Sci. 28, 34-49

18. Haynes, L., and Yau, K.-W. (1985) Nature 317, 61-64

19. Hurwitz, R. L., Bunt-Milam, A. H., Chang, M. L., and Beavo, J. A. (1985) J. Biol. Chem. 260, 568-573

20. Flaherty, K. M., Zozulya, S., Stryer, L., and McKay, D. B. (1993) Cell 75, 709-716

21. Nunn, B. J. and Baylor, D. A. (1982) Nature 299, 726-728

22. Nunn, B. J., Schnapf, J. L. and Baylor, D. A. (1984) Nature 309, 264-266

Chapter 2

Photoreceptor Protein s26,

a Cone Homologue of S-modulin

Introduction

On light absorption, vertebrate rods hyperpolarize through a well characterized phototransduction cascade (1-3). Photoreceptors not only respond to on and off of light, but also adapt to environmental light. The underlying mechanism of light adaptation has been shown to be the decrease in the intracellular Ca^{2+} concentration in the rod outer segment during light. Frog S-modulin and its bovine homologue, recoverin (5), inhibit the phosphorylation of the light activated rhodopsin at high Ca^{2+} concentration (6, 7). Rhodopsin phosphorylation is the shutoff mechanism of light activated rhodopsin. Therefore, the Ca^{2+}-dependent inhibition of rhodopsin phosphorylation probably contributes to increase in the light sensitivity of a rod photoreceptor during dark adaptation by increasing the lifetime of light activated rhodopsin. Recent studies showed that S-modulin family proteins are expressed in several nervous tissues.

A protein named s26 (small 26-kDa protein) was found during purification of S-modulin (12). The molecular characteristics of s26 are similar to those of S-modulin in several aspects. For example, their apparent molecular weights are slightly different but close to 26-kDa on the SDS-PAGE gel and they both bind to a hydrophobic column, phenyl-Sepharose, in a Ca^{2+}-dependent manner (12). The major difference is that s26 is eluted from a DEAE column at higher salt concentrations than S-modulin. These results raised the possibility that s26 is either a chemically modified form of S-modulin or a molecule different from S-modulin having a similar or different function in photoreceptors or other cells in frog retina. A chicken photoreceptor protein, visinin, has been reported to be present in cones (13) and have similar activity as S-modulin (14). Therefore, one possibility is that visinin is a cone homologue of S-modulin and

that s26 is frog visinin. However, the possibility that visinin is the cone homologue has been questioned because only the recoverin immunoreactivity has been found in both rods and cones in mammals (5, 15-17). Another possibility is that s26 localizes in some bipolar cells, because a recoverin-like protein is suggested to be present in these cells in human and monkey retina (17). In the present study, to clarify these points, I cloned cDNAs encoding s26, and examined the localization of s26 in frog retina.

Experimental Procedure

Determination of Partial Amino Acid Sequence of s26 – Purified s26 was digested with lysyl endopeptidase (Wako) according to the manufacture's protocol. The peptide fragments were isolated by reversed phase HPLC (C_{18} ODS column, Nakarai) by applying 0-100 % gradient of 80% CH_3CN in the presence of 0.1% trifluoroacetic acid. Major peak fractions were collected (Fig. 2-1), and the amino acid sequences of these peptides were analyzed by a protein sequencer (Applied Biosystem model 473A).

Isolation of cDNA Clones of s26 – The cloning strategy of s26 cDNA is illustrated in Figure 2-2. I synthesized degenerate oligonucleotides corresponding to the region between site specific to s26 and that conserved among S-modulin, visinin, and recoverin (see Results). The synthesized oligonucleotides were used as the primers for PCR. The PCR products were then used for the search of cDNA encoding s26. Since the full-length cDNA of s26 was not found in our cDNA library, RACE-PCR (18, 19) was applied to determine the complete nucleotide sequence at both ends. In this PCR, frog retinal cDNA was prepared according to an ordinary method (20), and RVF1

(CGAAGCTTCATCTAACCTCTTCAGGG) and RVR1 (CGAAGCTTGGAGGGATCATCT TGATT) primers were used for amplification of the 3' and the 5' regions, respectively (21).

Antibody Production – A Japanese White rabbit was immunized by a synthetic peptide of s26. An s26 peptide (see Result) was conjugated with maleimide-activated KLH (Pierce) through cysteine attached to the amino terminus of the peptide. Anti-s26 peptide antibody was affinity purified by its elution from a Western blot of purified s26. Anti-S-modulin antibody was raised against S-modulin in a mouse. Due to cross-reactivity of this antibody with s26, S-modulin antibody was preabsorbed by s26 before use.

Immunohistochemistry – Frogs were dark-adapted for at least 2 h, and the retina was removed with the aid of IR converter. A piece of the retina was fixed in the dark overnight at 4℃ either with Omni Fix (Xenetics Biomedical Inc.) or Bodian II solution (70% ethanol, 5% acetic acid and 5% formaldehyde) and then cryosectioned. Immunoreactivity of anti-s26 antibody was detected by fluorescein isothiocyanate-labeled anti-rabbit IgG antibody (Zymed Laboratories Inc.) and anti-S-modulin antibody by Texas Red-labeled anti mouse IgG antibody (Zymed Laboratories Inc.). Fluorescence was detected using a confocal microscope (Bio-Rad MRC 500 and MRC 600).

Evolutionary Distance Analysis among S-modulin Family Proteins – Evolutionary distance of the sequence (k) were calculated for 192 amino acids in the regions from Met-1 to Val-192 of s26. In this calculation, I used the proportion value (p) determined for the two amino acids and took multiple substitution into consideration with an

equation of $K = -\ln(1-p-p^2/5)$ (22). A phylogenetic tree was constructed by the neighbor-joining method (23) using chicken VILIP (24), bovine neurocalcin (25), and human hippocalcin (26) as outgroups.

Result

Amino Acid Sequence of s26 – Our preliminary study showed that the N terminus of s26 is blocked. For this reason, partial amino acid sequence were first determined in the proteolyzed fragments of s26. Purified s26 was digested with lysyl endopeptidase, and the peptide fragments were isolated by reversed phase HPLC (peak *a-f* in Fig. 2-2). The amino acid sequences of the six peptides were analyzed by a protein sequence analyzer (inset *a-f* at the top of Fig. 2-1). The result showed that the partial amino acid sequence of s26 is similar but definitely different from that of S-modulin, which showed that s26 is a protein distinct from S-modulin.

The amino acid sequence data of the six peptides were compared with those of S-modulin. Based on this comparison, PCR amplification of a partial cDNA clone of s26 was attained between two regions, one determined in peptide *a* (*large dots* in Fig. 2-3) and the other having consensus amino acid sequence among S-modulin, recoverin, and visinin (*small dots* in Fig. 2-3). Degenerate oligonucleotides corresponding to those regions were synthesized and used as primers. The PCR product was then used for the search of cDNAs encoding s26. The results, however, showed that our frog retinal cDNA library does not contain the full-length cDNA of s26. Then, RACE-PCR method was applied to determine the 5' and the 3' ends of cDNA of s26. A primer RVF1 (Fig. 2-3 arrow indicated by $*$) was used for determination of the 3'

region and RVR1 (arrow indicated by * *) of the 5' region (see "Experimental Procedure").

Fig. 2-3 shows the nucleic acid and deduced amino acid sequences of s26. The first ATG is followed by an open reading frame of 588 bases and fulfills the Kozak criteria for the initiation signal in eukaryote (27). As this ATG being the translational initiation codon, this cDNA encodes 196 amino acids.

As underlined in Fig. 2-3, the deduced amino acid sequence in the cDNAs contained all the sequences found in the six peptide fragments of s26 shown in Fig. 2-2. In addition, the calculated molecular mass was 22,818, which is close to the molecular mass of s26 estimated by SDS-PAGE. I, therefore, concluded that these cloned cDNAs encode s26.

In Fig. 2-4, the amino acid sequence of s26 was compared with those of S-modulin (7) and visinin (13). Similarly as in S-modulin and visinin, s26 contains three putative EF hand structures (Fig. 2-4, dotted lines). However, EF1 might be defective because of the cysteine residue in this structure, and EF2 and EF3 are probably the actual Ca^{2+}-binding sites (28). The N-terminal region of s26 has a consensus N-terminal myristoylation site (GXXXS; Italic) (29); therefore, the terminal methionine would be cleaved, and the N-terminal glycine is modified by lipids. This idea is consistent with our finding that the N terminus of s26 is resistant to Edman degeneration. Even though both s26 and S-modulin are found in frog retina, the amino acid sequence of s26 shows only 67% identity to S-modulin but 77% identity to visinin, a Ca^{2+}-binding protein reported to be present in chicken cones (Table 2-1). The evolutionary distances calculated from the sequence data showed that s26 is a closer member to visinin than S-modulin (Fig. 2-5).

Localization of s26 in Frog Retina – Rabbit anti-s26 antibody was obtained to

examine the localization of s26 in frog retina. S-modulin and s26 are both present in frog retina, and their amino acid sequences are similar. Therefore, a highly specific s26 antibody is required. An antibody was raised against a synthetic peptide whose amino acid sequence is specific to s26 (Gln-174 to Met-183; underlined in Fig. 2-4). This antibody did not cross-react with S-modulin on the Western blot (Fig. 2-6, middle three lanes).

Localization of s26 in frog retina was detected by fluorescence attached to secondary antibody. Immunoreactivity of anti-s26 antibody was present in the photoreceptor layer in frog retina but not in other layers (Fig. 2-7 A). A magnified picture indicated that cones are immunoreactive but rods are not (Fig. 2-7 B). The result, therefore, showed that s26 is expressed in cone photoreceptors. The immunoreactivity of s26 distributed uniformly within a cell. By comparing a transmission image with a fluorescence image, it was found that most of the immunoreactive cells had oil droplets and the cells having oil droplets were mostly immunoreactive.

We also tried to obtain an anti-S-modulin antibody against a synthetic peptide of the corresponding region of S-modulin to examine the localization of S-modulin. However, the attempt failed. As an alternative, I obtained a polyclonal anti-S-modulin antibody raised against S-modulin whole protein. This antibody recognized both S-modulin and s26 (data not shown); for this reason, the S-modulin antibody was preabsorbed by s26 before use. This partially purified S-modulin antibody recognized S-modulin but not s26 on the Western blot (Fig. 2-6, right three lanes) and stained mainly the photoreceptor layer (Fig. 2-7 C). Since the cell body of a rod is present at the outer half of the outer nuclear layer (onl in Fig. 2-7), the immunoreactive cells were judged as rods (Fig. 2-7 D).

Discussion

In the present study, the cDNAs of s26 were cloned, and the deduced amino acid sequence showed a higher homology to visinin (Fig. 2-4 and 2-5, Table 2-1). Immunohistochemical analysis showed that the immunoreactivity of anti-s26 antibody was found in cones (Fig. 2-7). It was indicated that the purified s26 inhibited phosphorylation of rhodopsin at high Ca^{2+} concentrations as S-modulin does (30). These results showed that s26 is frog visinin and is a cone homologue of S-modulin in frog retina. In addition, the immunoreactivity against anti-S-modulin antibody was found in rods (Fig. 2-7).

Rod-and-cone Cell-type Specific Expression of S-modulin Homologue – The present study showed that s26 is present in cones and S-modulin in rods in frog retina. This is the first demonstration that a different set of the S-modulin homologues is expressed in the same retina in a cell-type specific manner. The rod-and-cone cell-type specific expression is generally observed in the proteins involved in the phototransduction. For example, besides visual pigments, arrestin (31, 32), transducin (33, 34), cGMP phosphodiesterase (35, 36), cGMP-gated channel (37) are expressed in a cell-type specific manner. In this sense, the result in the present study is consistent with previous studies. In mammalian retina, however, cone homologues of S-modulin have not been found. Namely, immunoreactivity of anti-recoverin antibody was found in both rods and cones in human, monkey, bovine and rat retinas (5, 15-17). Furthermore, immunoreactivity against an antibody specific to chicken visinin has not been found in human and bovine retina (16), and an attempt to isolate visinin from bovine retina was not successful (16). In mammals, therefore, recoverin might be expressed

exceptionally in both rods and cones. However, the cone homologue may have not been detected because the cone homologue has high homology to recoverin and differs significantly from chicken visinin in its amino acid sequence.

The present study suggests that cell-type specific expression of S-modulin homologue is also present among cone cells in frog retina. In frog retina, three kinds of cone cells are present (38): single cones and double cones consisting of principal and accessory member. Single cones and the principal member of the double cone have oil droplets, but the accessory member does not. In the present study, most of the cones immunoreactive to anti-s26 antibody possessed oil droplets and inversely, cones having oil droplets were mostly immunoreactive to s26 antibody (see "Result"). These observations suggest that s26 is present in both single cones and the principal member of the double cone but not in the accessory member. In agreement with this view, microspectrophotometry has shown that the absorption maximum of the visual pigment in single cones is the same as that in the principal member but differs from that in the accessory member (39). The above consideration, therefore, suggests that another S-modulin-like protein is present in the accessory member of the double cone in frog retina.

In frog retina, another type of rod photoreceptor, green rods are present. Unfortunately, it was not clear in the present study whether green rods have the same S-modulin as red rods.

Function of s26 – As shown by Kawamura *et al* (30), s26 inhibits the phosphorylation reaction of rhodopsin at high Ca^{2+} concentrations. This observation is consistent with the previous finding that visinin and recoverin have the same effect on the prolongation of a photoresponse in gecko rods (14). S-modulin in frog rods has been postulated to be a Ca^{2+}-dependent regulator of rhodopsin phosphorylation (6). Similarly, as

S-modulin does, s26 would regulate the phosphorylation reaction of cone visual pigments in a Ca^{2+}-dependent manner.

Distribution of s26 and S-modulin in a Cell – According to the postulated function of s26 and S-modulin, these proteins are expected to be present in the outer segment. However, it does not seem to be the case for two lines of evidence. One is that immunoreactivities against s26 and S-modulin antibodies distributed throughout the cell (Fig. 7). This observation agrees with the previous studies done by others (5, 15, 16). However, this result does not always mean that these proteins distribute throughout the cell under *in situ* condition. Since S-modulin and s26 are essentially soluble, these proteins may diffuse from the outer segment to other parts of the cell during fixation. This possibility, however, is excluded by the second line of the evidence that the molar ratio of s26 to S-modulin is much higher than that of their corresponding visual pigments. The molar ratio of cone to rod visual pigment could be an indicative of the volume ratio of their outer segments. For this reason, if s26 and S-modulin are present exclusively in the outer segment, the molar ratio of s26/S-modulin should be similar as that of cone/rod visual pigment. According to the microspectrophotometric measurement in the retina of a frog (*Rana pipiens*), the molar ratio of cone visual pigment to that of rod visual pigment (rhodopsin) is ~0.2/10 (38), while s26 /S-modulin ratio was ~7/10 in the present study (see "Results"). The population of cones is almost equal to that of rods in frog retina (39), and the sizes of their inner segment and cell body of a cone are not so different from those of a rod (rough estimation from electron micrographs in Ref. 38). For this reason, the ratio of s26/S-modulin (~7/10 in this study) could be explained by uniform spatial distribution of s26 and S-modulin in cones and rods, respectively.

The uniform distribution of these proteins may mean that these proteins not only

inhibit phosphorylation of visual pigment but also have some other function(s) in other part of the cell. Alternatively, the uniform distribution may just reflect that these proteins are essentially soluble. Further studies are required to solve this issue.

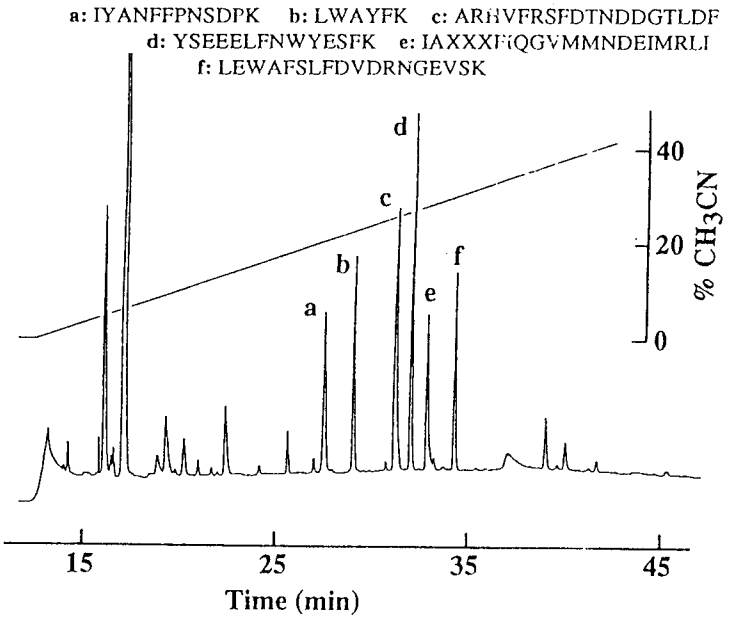

Figure 2-1: Separation of proteolyzed s26 fragments by reversed phase HPLC and their amino acid sequences. Purified s26 was digested with lysyl endopeptidase. The proteolytic fragments were isolated by reversed phase HPLC. Amino acid sequences of the six major peptides (*a-f*) are shown (upper inset).

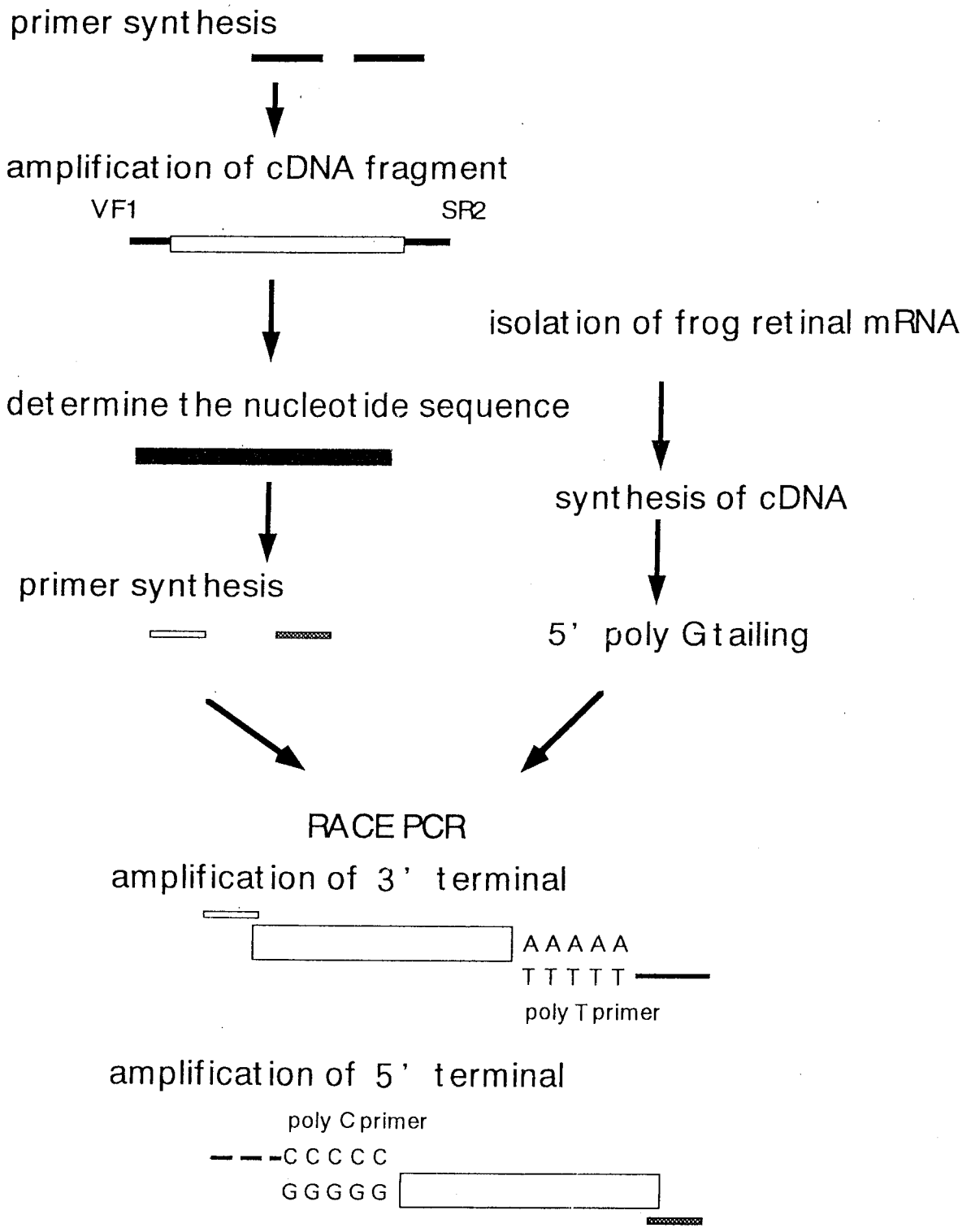

Figure 2-2: Cloning strategy of cDNA coding s26.

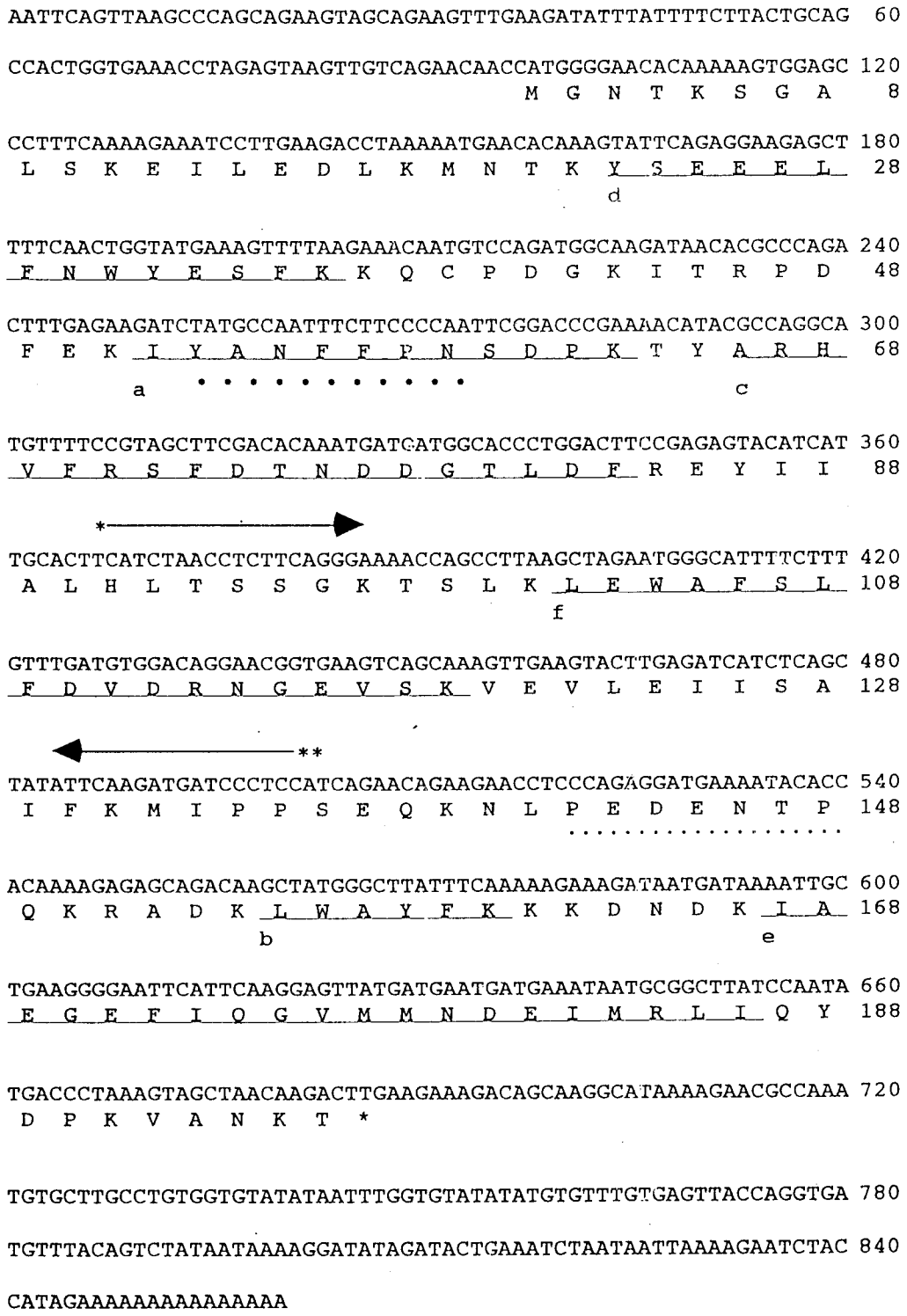

Figure 2-3: cDNA and deduced amino acid sequence of s26. Large and small dots indicate the regions used as the primers in PCR. Arrows indicate the primers used for RACE-PCR; one (*) for determination of the 3' end and the other (* *) of the 5' end. The sequences in the six peptides obtained by reversed phase HPLC are found in this sequence (*a-f* as in Fig. 2).

Figure 2-4: Alignment of amino acid sequences of S-modulin, s26, and visinin. A colon shows identical amino acid and dotted lines EF hand structures. *Italic* (Gly-2 to Ser-6) shows a consensus N-terminal myristoylation site, and a line (Gln-174 to Met-183) shows the sequence used for generation of anti-s26 antibody.

	S-modulin	Recoverin	Visinin	s26
	%	%	%	%
S-modulin	100	83	61	66
Recoverin		100	59	66
Visinin			100	77
s26				100

TABLE 2-1: Amino acid sequence identities among frog S-modulin, bovine recoverin, chicken visinin, and frog s26

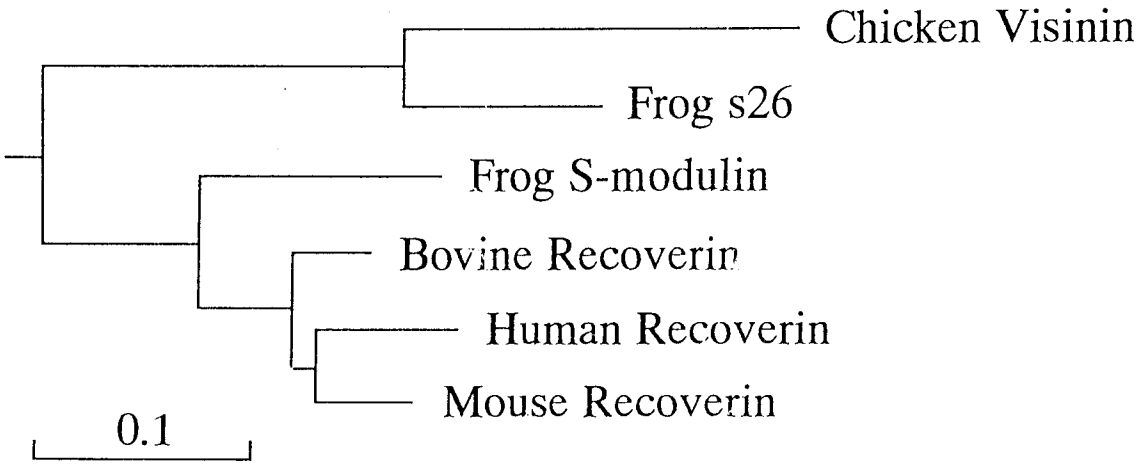

Figure 2-5: A phylogenetic tree of S-modulin protein family. According to the reported sequences of the proteins shown, evolutionary distances of the sequences were calculated. The sequences used were those of visinin (13), S-modulin (7), bovine recoverin (5), human recoverin (40), and mouse recoverin (41). Bar indicates 10% replacement of an amino acid per site (k = 0.1; see "Experimental Procedure").

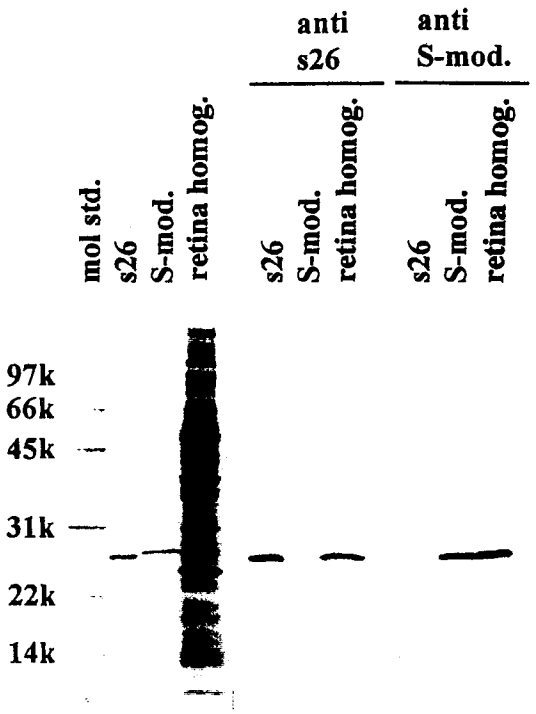

Figure 2-6: Western blot analysis of antibodies raised against an s26 peptide and S-modulin molecule. Purified s26 (s26), S-modulin (S-mod.), and retinal homogenate (retina homog.) were subjected to SDS-PAGE and then transferred to a nylon membrane. The transferred proteins were stained with Coomasie Brilliant Blue (left three lanes) or subjected to Western blot analysis by the anti-s26 (middle three lanes) and the anti-S-modulin antibodies (right three lanes). Immunoreactivity was detected by the ABC method and visualized with horseradish peroxidase-diaminobenzidine reaction.

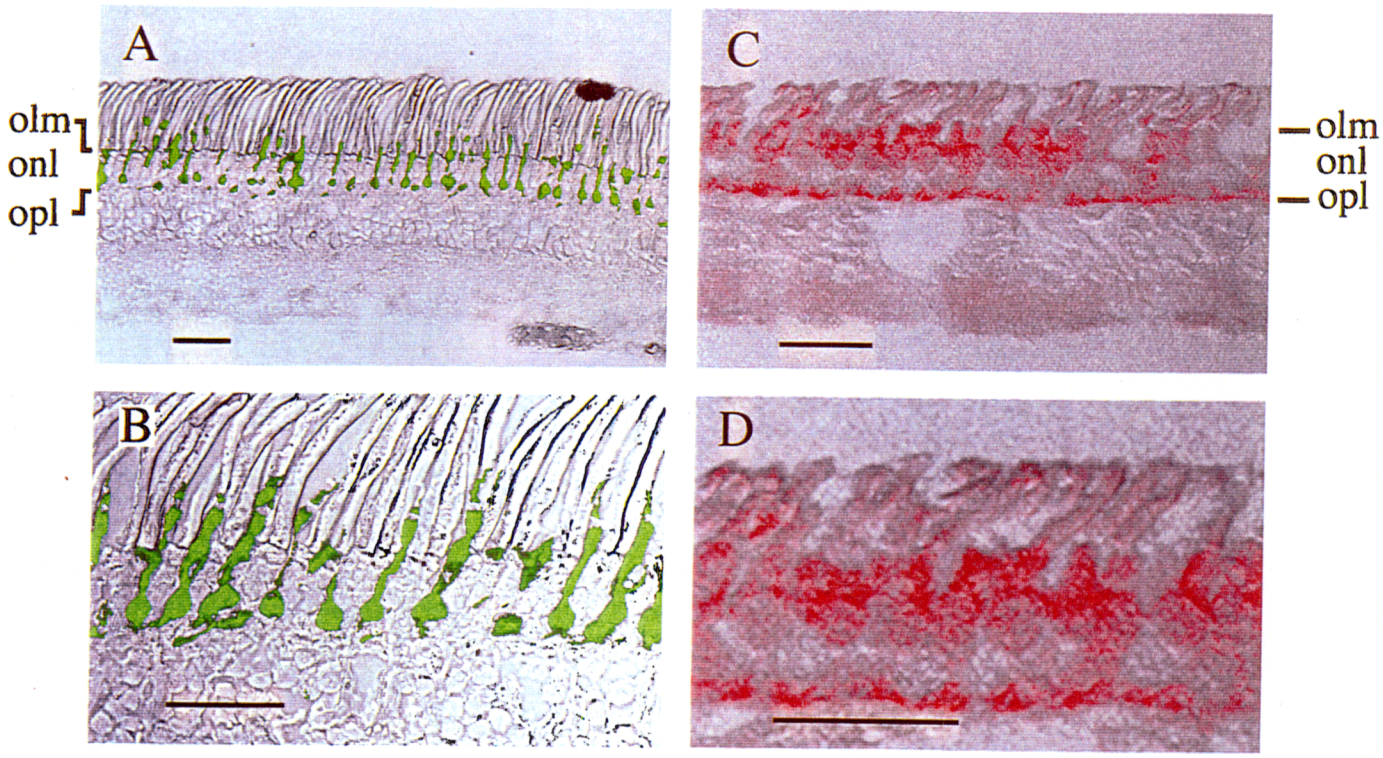

Figure 2-7: Immunofluorescent staining of frog retina with the anti-s26 and the anti-S-modulin antibodies. A and B, staining with the s26 antibody at low and high magnification, respectively. C and D, staining with the S-modulin antibody at low and high magnification, respectively. Each bar in the figure shows 50 μm; olm, outer limiting membrane; onl, outer nuclear layer; opl, outer plexiform layer. Fluorescence image was superimposed on the transmission image.

References

1. Stryer, L. (1991) J. Biol. Chem. 268, 10711-10714

2. Lagnado, L., and Baylor, D. A. (1992) Neuron 8, 955-1002

3. Kawamura, S. (1995) Neurobiology and Clinical Aspects of the Outer Retina (Djamgos, D. M. B. A., Archer, S. N., and Vallerga, S., eds) pp. 105-131, Chapman & Hall, London

4. Kawamura, S., and Murakami, M. (1991) Nature 349, 420-423

5. Dizhoor, A. M., Ray, S., Kumar, S., Niemi, G., Spencer, M., Brolley, D., Walsh, K. A., Philipov, P. P., Hurley, J. B., and Stryer, L. (1991) Science 251, 915-918

6. Kawamura, S. (1993) Nature 362, 855-857

7. Kawamura, S., Hisatomi, O., Kayada, S., Tokunaga, F., and Kuo, C.-H. (1993) J. Biol. Chem. 268, 14579-14582

8. Palczewski, K., Buczylko, J., Lebioda, L., Crabb, J. W., and Polans, A. S. (1993) J. Biol. Chem. 268, 6004-6013

9. Chen, J., Makio, C. L., Peachey, N. S., Baylor, D. A., and Simon, M. I. (1995) Science 267, 374-376

10. Kawamura, S. (1994) Neurosci. Res. 20, 293-298

11. DeCastro, E., Nef, S., Fiumelli, H., Lenz, S. E., Kawamura, S., and Nef, P. (1995) Biochem. Biophys. Res. Commun. 216, 133-140

12. Kawamura, S. (1992) Photochem. Photobiol. 56, 1173-1180

13. Yamagata, K., Goto, K., Kuo, C.-H., Kondo, H., and Miki, N. (1990) Neuron 2, 469-476

14. Gray-Keller, M., Polans, A. S., Palczewski, K., and Detwiler, P. B. (1993) Neuron 10, 523-531

15. Polans, A. S., Buczylko, J., Crabb, J., and Palczewski, K. (1991) J. Cell. Biol. 112, 981-989

16. Polans A. S., Burton, M. D., Haley, T. L., Crabb, J. W., and Palczewski, K. (1993) Invest. Ophthal. Vis. Sci. 34, 81-90

17. Milam, A. H., Dacay, D. M., and Dizhoor, A. M. (1993) Vis. Neurosci. 10, 1-12

18. Frohman, M. A., Dush, M. K., and Martin, G. R. (1988) Proc. Natl. Acad. Sci. U.S.A. 85, 8998-9002

19. Ohara, O., Dorit, R. L., and Gilbert, W., (1989) Proc. Natl. Acad. Sci. U.S.A. 86, 5673-5677

20. Maniatis, T., Frisch, E. F., and Sambrook, J. (1982) Molecular Cloning; A Laboratory Manual, Cold Spring Harbor Laboratory, Cold Spring Harbor, NY

21. Hisatomi, O., Iwasa, T., Tokunaga, F., and Yasui, A. (1991) Biochem. Biophys. Res. Commun. 174, 1125-1132

22. Kimura, M. (1983) The Neutral Theory of Molecular Evolution, Cambridge University Press, Cambridge, United Kingdom

23. Saitou, L., and Nei, M. (1987) Mol. Biol. Evol. 4, 406-425

24. Lenz, S. E., Henschel, Y., Zopf, D., Voss, B., and Gundelfinger, E. D. (1992) Mol. Brain. Res. 15, 133-140

25. Okazaki, K., Watanabe, M., Ando, Y., Hagiwara, M., Terasawa, M., and Hidaka, H. (1992) Biochem. Biophys. Res. Commun. 185, 147-153

26. Takamatsu, K., Kobayashi, M., Saitoh, S., Fujishiro, M., and Noguchi, T. (1994) Biochem. Biophys. Res. Commun. 200, 606-611

27. Kozak, M. (1986) Cell 44, 283-292

28. Flaherty, K. M., Zozulya, S., Stryer, L., and Mckay, D. B. (1993) Cell 75, 709-716

29. Towler, D. A., and Gordon, J. I. (1988) Annu. Rev. Biochem. 57, 69-99

30. Kawamura, S., Kuwata, O., Yamada, M., Matsuda, S., Hisatomi, O., and Tokunaga,, F. (1996) J. Biol. Chem. 271, 21359-21364

31. Nir, I., and Ransom (1992) J. Histochem. Cytochem. 40, 343-352

32. Craft, C. M., Whitmore, D. H., and Wiechmann, A. F. (1994) J. Biol. Chem. 269, 4613-4619

33. Lerea, C. L., Somers, D. E., Hurley, J. B., Klock, I. B., and Bunt-Milam, A. H. (1986) Science 234, 77-80

34. Peng, Y.-W., Robishaw, J. D., Levine, M. A., and Yau, K.-W. (1992) Proc. Natl. Acad. Sci. U.S.A. 89, 10882-10886

35. Charbonneau, H., Prusti, R. K., LeTrong, H., Sonnenburg, W. K., Mullaney, P. J., Walsh, K. A., and Beavo, J. A. (1990) Proc. Natl. Acad. Sci. U.S.A. 87, 288-292

36. Li, T., Volpp, K., and Applebury, M. L. (1990) Proc. Natl. Acad. Sci. U.S.A. 87, 293-297

37. Bonigk, W., Altenhofen, W., Muller, F., Dose, A., Illing, M., Molday, R. S., and Kaupp, U. B. (1993) Neuron 10, 865-877

38. Nilsson, S. E. G. (1964) J. Ultrastruct. Res. 10, 390-416

39. Liebman P. A., and Entine, G. (1968) Vision Res. 8, 761-775

40. Murakami, A., Yajima, T., and Inada, G. (1992) Biochem. Biophys. Res. Commun. 187, 234-244

41. McGinnis, J. F., Stepanik, P. L., Baehr, W., Subbaraya, I., and Lerious, V. (1992) FEBS Lett. 302, 172-176

Chapter 3

Functional Expression and Characterization of Frog Photoreceptor-Specific Calcium-Binding Protein

Introduction

In rod cells, light activates rhodopsin, which triggers the phototransduction cascade, resulting in the closure of cation channels. Ca^{2+} influx through this cation channel is then stopped, and consequently the intracellular Ca^{2+} concentration decreases. The light-activated rhodopsin is inactivated probably with phosphorylation by rhodopsin kinase, cGMP-gated cation channels are then opened, and the intracellular Ca^{2+} concentration is then restored to a high level. This change in the Ca^{2+} concentration has been suggested to be the underlying mechanism of the light-dark adaptation of vertebrate photoreceptor cells (1, 2). Kawamura and Murakami (3) found a photoreceptor-specific Ca^{2+}-binding protein, S-modulin (sensitivity-modulating protein), which controls the phosphorylation of light-activated rhodopsin in frog rods. S-modulin inhibits rhodopsin phosphorylation at high Ca^{2+} concentration (that is, in the dark-adapted state), but not at low Ca^{2+} concentration (light-adapted state) (4).

The visual transduction cascade in cones is less well understood than that in rods. However, cones are reported to have similar isozymes of phototransduction proteins, including the cGMP-sensitive channel (5, 6), opsins (7), transducin (8), and phosphodiesterase (PDE) (9). It was suggested that the basic signal transduction pathway of cones and rods is similar, even though cones are less sensitive than rods. In primates, cones require 100 times as many as photons to elicit a half maximal signal in comparison with rods (10). The time course of the light response is faster in cones than rods, and light adaptation is much more pronounced in cones than in rods (11). However, the biochemical bases underlying these physiological differences are still unclear.

In the chapter 2, I have reported the isolation of s26 cDNA, a homologue of

S-modulin, which exists in frog cones (12). The deduced amino acid sequence shows 68% and 77% identity with, respectively, S-modulin and chicken visinin, a cone-specific Ca^{2+}-binding protein. Functional expression of these recombinant proteins will provide useful tools for studying the molecular mechanism of adaptation in rods and cones. In this paper, we report the functional expression of S-modulin and s26 in *Escherichia coli* (*E. coli*), and the characterization of these photoreceptor -specific Ca^{2+}-binding proteins.

Experimental Procedure

Construction of expression vectors for S-modulin and s26 – The construction of expression vector for S-modulin is carried out as shown in Figure 3-1. S-modulin cDNA was cloned into a plasmid vector as described by Kawamura et al. (13), and used as the template for polymerase chain reactions. The coding region of S-modulin was amplified using as primers SMD-NTF (5'-CGCCCGGGCTCGAGCCACCATGGG TAACACCAA-3') and SMD-CTR (5'-GCGTCGACTCGAGCTAGTGTTTTT-3') (14), inserted between the NcoI and BamHI sites of a pET-16b (Novagen) plasmid vector (forming vector pET-Smd).

The construction method of expression vector for s26 is summarized in Figure 3-2. s26 cDNA was isolated and cloned into a pUC18 plasmid vector as described in Kawamura et al. (12). To make additional restriction sites in the 3' end of the s26 coding region (for insertion into a pET-16b vector), 40 cycles (94-50-72 °C) of amplification were carried out, using a frog retinal cDNA as the template and s26-F3 (5'-TGATAAAATTGCTGAAGG-3') and s26-CTR (5'-CCTAAGCTTGGATCCTCAAGTCT

TGTTAGC-3') as primers. The amplified 3' fragment was cloned and ligated with a 5' (PstI-EcoRI) fragment of s26. The coding region of s26 was then inserted between the NcoI and BamHI sites of a pET-16b plasmid vector (forming vector pET-s26).

Expression of eS-modulin and es26 in E. coil. – In this paper, S-modulin and s26 expressed in *E. coli* are designated eS-modulin and es26, respectively, to discriminate them from the native S-modulin and s26 isolated from frog retinas. BL21(DE3) cells were transformed with pET-Smd or pET-s26. Cells were pre-cultured in 10-50 ml of Luria-broth (LB) medium containing 50 μg/ml of ampicillin at 37°C for 4-5 h, and were then added to 1 l of LB medium. After optical density at 600 nm reached 0.6-1.0 (about 3-4 h later), 1 mM (final concentration) of isopropyl-β-*D*-thiogalactopyranoside (IPTG) was added to the medium, and the cells were further cultured for 8-12 h.

For the expression of myristoylated S-modulin and s26, BL21(DE3) cells previously transformed with pBB131 (kindly provided by Prof. Jeffrey I. Gordon; an expression vector of *N*-myristoyl transferase), were co-transformed with pET-Smd or pET-s26 (15). Cells were cultured in LB medium containing ampicillin and kanamycin (final concentration 50 μg/ml each), and 50 μM (final) of myristic acid was added to the culture medium 1 h before the addition of IPTG.

E. coli cells were harvested by centrifugation (2,700 xg for 15 min), washed with 0.9% NaCl aqueous solution and recentrifuged. The pellet was suspended in 100 ml of lysis buffer (50 mM Tris-HCl, 200 mM KCl, 1 mM DTT, 1 mM EDTA, 0.1 mg/ml phenylmethylsulfonylfluoride, pH 8.0), and incubated at 0°C for 30 min. The lysates were then sonicated 5 times for 5 min, with intervals of 5 min on ice, and centrifuged at 6,500 xg for 30 min.

Purification of eS-modulin and es26 – The purification methods of eS-modulin and es26 are shown in Fig.3-3. eS-modulin expressed in BL21(DE3) cells was mainly found in the insoluble fraction. Cell debris from centrifugation was suspended in 200 ml of buffer A (50 mM Tris-HCl, 50 mM KCl, 5 mM EGTA, 5 mM DTT, pH 8.5) containing 8 M urea, and the soluble fraction was then isolated by recentrifugation. In order to remove urea, the supernatant was dialyzed stepwise (3h each) against buffer A containing 4 M urea, buffer A containing 2 M urea, and then buffer B (50 mM Tris-HCl, 1 mM DTT, 1 mM EGTA, pH 8.0, 50 mM KCl). A small amount of precipitated protein was removed by recentrifugation.

The centrifugal supernatant from the dialysate was applied to a DEAE-Sephadex (Pharmacia) column equilibrated with buffer B, and the recombinant proteins were eluted with a linear gradient of 0.05-1M KCl in buffer B. The fractions containing eS-modulin were dialyzed against buffer C (50 mM HEPES, 1 mM DTT, pH 7.5) containing 500 mM KCl and 5 mM $CaCl_2$ at 4° C for 3 h, and applied to a phenyl-Sepharose (Pharmacia) column equilibrated with buffer C. eS-modulin was eluted with buffer C containing 50 mM KCl and 5 mM EGTA, and stored at 4° C until use. The refolding and purification protocols of es26 were performed likewise.

Phosphorylation assay – Rhodopsin in ROS (rod outer segment) membranes of frog retinas washed with the low (1nM) Ca^{2+} buffer, was bleached in the presence of [γ-^{32}P] ATP and the exogenous recombinant proteins (4). After separation by sodiumdodecylsulfate polyacrylamide gel electrophoresis (SDS-PAGE), the radioactivity of ^{32}P incorporated into the bleached rhodopsin was measured by Cerenkov counting and densitometric analysis of the autoradiographs.

Spectroscopic measurements – The amounts of purified eS-modulin and es26 were quantified by spectrophotometrical measurement at 280 nm using the specific absorbance ($E_{1mg/ml}$ = 1.9). Fluorescence emission spectra were recorded from 300 to 400 nm by a fluorescence spectrophotometer (Hitachi, F-4500) with an excitation wavelength at 290 nm, in mixtures containing 2 μM recombinant protein, 100 mM KCl, 5 mM 2-mercaptoethanol, 1 mM EGTA, 100 mM HEPES (pH 7.0) and $CaCl_2$ of various concentrations, adjusted with the Ca^{2+}/EGTA buffers described by Sitaramayya and Margulis (16). Free Ca^{2+} concentration in the buffers was determined by using the fluorescent indicator Fura-2 (17). Circular dichroism (CD) spectra were measured by a CD spectrophotometer (Jasco, CD-J600), using mixtures containing 10 μM recombinant protein, 20 mM KCl, 10 mM HEPES and 4 mM DTT (pH 7.0), in the presence of 1 mM EGTA or 0.5 mM $CaCl_2$.

Results

Expression and purification of eS-modulin and es26 – For the high-level expression of eS-modulin, I constructed an expression vector, pET-Smd, and transformed BL21(DE3) cells with the vector. Judging from the SDS-PAGE pattern stained with Coomassie brilliant blue (CBB), the amount of eS-modulin was estimated to comprise more than 30% of the total protein (Fig. 3-4, lane 1). Although the native S-modulin being a soluble protein, eS-modulin was found in the insoluble fractions (Fig. 3-4, lane 2) and was considered unlikely to have the native conformation. Therefore, we solubilized it with buffer A containing 8 M urea, and refolded the protein by three steps of sequential dialyses (see Experimental procedures). This stepwise dialysis was

required to avoid aggregation induced by the dialysis of the 8M urea solution directly against buffer B. The centrifugal supernatant from the dialysate was applied to a DEAE-Sephadex column. Similar to native S-modulin isolated from frog retinas, eS-modulin was found in the pass-through fraction (Fig. 3-4a, lane 3). The eS-modulin fraction was further purified with a phenyl-Sepharose column, and the resulting eS-modulin showed a single band on SDS-PAGE analysis (Fig. 3-4a, lane 4). We ordinarily obtained 20-50 mg of purified eS-modulin from 1 l of culture. es26 was purified in the same way, except for the DEAE-Sephadex column step, where es26 was eluted with buffer B containing 400 mM KCl (Fig. 3-4b, lane 3).

The amino acid compositions of eS-modulin and es26 showed values reasonably close to those calculated from their amino acid sequences. The N-terminal amino acid sequences of eS-modulin and es26 expressed without pBB131 were directly confirmed by peptide sequencing. N-terminal myristoylation was suggested by the fact that the N-termini of eS-modulin and es26 expressed with pBB131 were blocked against the Edman degradation (myristoylated and unmyristoylated recombinant proteins are discriminated by the notations (+myr) and (-myr), respectively). The existence of myristoyl groups in the N-termini of eS-modulin (+myr) and es26 (+myr) was further confirmed by the fact that the retention time from a C-18 column for the (+myr) species was longer than that for the (-myr) species. Judging from HPLC patterns, the presence of (-myr) species in purified eS-modulin (+myr) or es26 (+myr) samples, if present, was less than 1 % (data not shown).

Physicochemical properties of eS-modulin and es26 – Figure 3-5 shows the inhibition of rhodopsin phosphorylation in the presence of eS-modulin and es26. Both (+myr) and (-myr) species of eS-modulin and es26 (+myr) inhibited the phosphorylation at a high (10 μM) Ca^{2+} concentration, as do native S-modulin and s26

isolated from frog retinas (4, 12).

The CD spectra of these proteins indicated helical structures because they exhibited the typical pattern of a a-helix with paired troughs at 208 and 222 nm. The effects of the myristoylation were observed on the CD spectra of eS-modulin (Fig. 3-6). In the region from 200 to 250 nm, the CD spectra of (+myr) and (-myr) species of eS-modulin had different profiles in the absence of Ca^{2+} (Fig. 5a, solid line), but those of es26 showed less difference (Fig. 3-6b). The CD spectra of both (+myr) and (-myr) of both proteins species were almost the same in the presence of 0.5 mM Ca^{2+}. In all cases, negative peaks around 222 nm were enlarged in the presence of Ca^{2+}, suggesting that the a-helical content of these proteins was increased by binding Ca^{2+}. Similar CD spectral changes were observed in our analysis of bovine recoverin (18). It seems that these Ca^{2+}-binding proteins undergo similar structural changes when they bind Ca^{2+}.

N-terminal myristoylation also affected the tryptophan emission spectra of eS-modulin (Fig. 3-7a) and es26 (Fig. 3-7b). eS-modulin (+myr) showed emission maxima at 322 in the absence of Ca^{2+}, and shifted their maxima to a longer wavelength 337 by increasing Ca^{2+} concentration to 1 mM. eS-modulin (-myr) had emission maxima at 332 and 340 nm in the absence and presence of Ca^{2+}, respectively. In the case of es26, emission maxima of (+myr) and (-myr) species appeared to be at 324 and 331 nm, respectively, and also underwent red-shifts (at 334 and 336 nm, respectively) by increasing free Ca^{2+}. Similar emission spectra were reported for (+myr) and (-myr) species of recombinant recoverin, which had maxima at 333 and 339 nm, respectively, in the absence of Ca^{2+}. Emission maxima of both (+myr) and (-myr) species of recoverin underwent red-shift to at 339 nm in the presence of Ca^{2+} (19). The half maximal Ca^{2+} concentrations of the emission changes at 370 nm were estimated at 0.73 μM for eS-modulin (+myr) and 0.67 μM for es26 (+myr) (Fig. 3-7c). Similar values

were calculated on monitoring either wavelength or integration of emission intensity from 350 to 400 nm.

Discussions

es26 (+myr) inhibited rhodopsin phosphorylation to almost the same extent as eS-modulin (+myr) (Fig. 3-5). This indicates that s26 is involved in the adaptation mechanism in cones, that is, by binding to the cone outer segment membrane, inactivates cone kinase (if it exists) and inhibits phosphorylation of cone pigments.

Recoverin is thought to bind two Ca^{2+} ions per molecule (20). In our preliminary experiments by the rapid flow dialysis method (21), both eS-modulin and es26 were shown to bind two Ca^{2+}. The peptide segments of S-modulin and s26 corresponding to the EF-2 and EF-3 regions of recoverin may bind Ca^{2+}. The half-maximal Ca^{2+} concentrations of bovine recoverin, which affect binding to phenyl agarose resin and the inhibition of rhodopsin phosphorylation, are reported to be 1.0 μM and 0.56 μM, respectively (22, 23). These are close to the values obtained for eS-modulin and es26 in the present experiments of the half-maximal emission changes (about 0.7 μM). S-modulin and s26 seem to have similar Ca^{2+}-dependent physical properties irrespective of their localization in the retina. However, some difference between es26 and eS-modulin was found in response to the change of the local environment; that is, the Ca^{2+}-bound form of eS-modulin showed a slightly larger shift of the emission maximum than that of es26. Furthermore the CD spectral changes induced by Ca^{2+} concentrations also showed some difference between S-modulin and s26 (Fig. 3-6). It is not yet clear if these differences have some relationship with the physiological

differences between rods and cones.

A variety of proteins with diverse biological activities have their N-termini linked to fatty acids such as myristic acid (24). The (-myr) species of eS-modulin inhibited rhodopsin phosphorylation to almost the same extent as the (+myr) species, but the fatty acid modification of S-modulin is more likely to influence the membrane binding properties (22, 25) rather than the direct interaction with target proteins (26, 27). However, it has been suggested recently that N-myristoylation of recoverin enhances its efficiency as an inhibitor of rhodopsin kinase (28, 29).

It has been suggested that the myristoyl group is in contact with hydrophobic residues, including tryptophan, of recoverin in the Ca^{2+}-free form and is exposed to solvent in the Ca^{2+}-bound form (30). This conformational transition of recoverin is not grossly affected by the presence or absence of myristoylation (30). Bovine recoverin, frog S-modulin and s26 have three conserved tryptophan residues at corresponding positions. The change of fluorescence emission spectra leads us to speculate on the Ca^{2+} dependent structural changes of S-modulin and s26 as follows. One or more tryptophan residues of both eS-modulin and es26, irrespective of the myristoylation, are in the more polar environments in the Ca^{2+}-bound form than in the Ca^{2+}-free form. The difference of the local environments between (+myr) and (-myr) species is larger in the Ca^{2+}-free form than in the Ca^{2+}-bound form. In these Ca^{2+}-binding proteins, the exposure of hydrophobic surfaces to solvent may play a more essential role in the inhibition of rhodopsin kinases than fatty acid modification of the proteins.

Our overexpression system of S-modulin or s26 with and without myristoylation should enable more detailed structural analyses, by providing large enough samples for multidimensional nuclear magnetic resonance spectroscopy and X-ray crystallography. It may provide informations to understand the physiological differences between rods and cones.

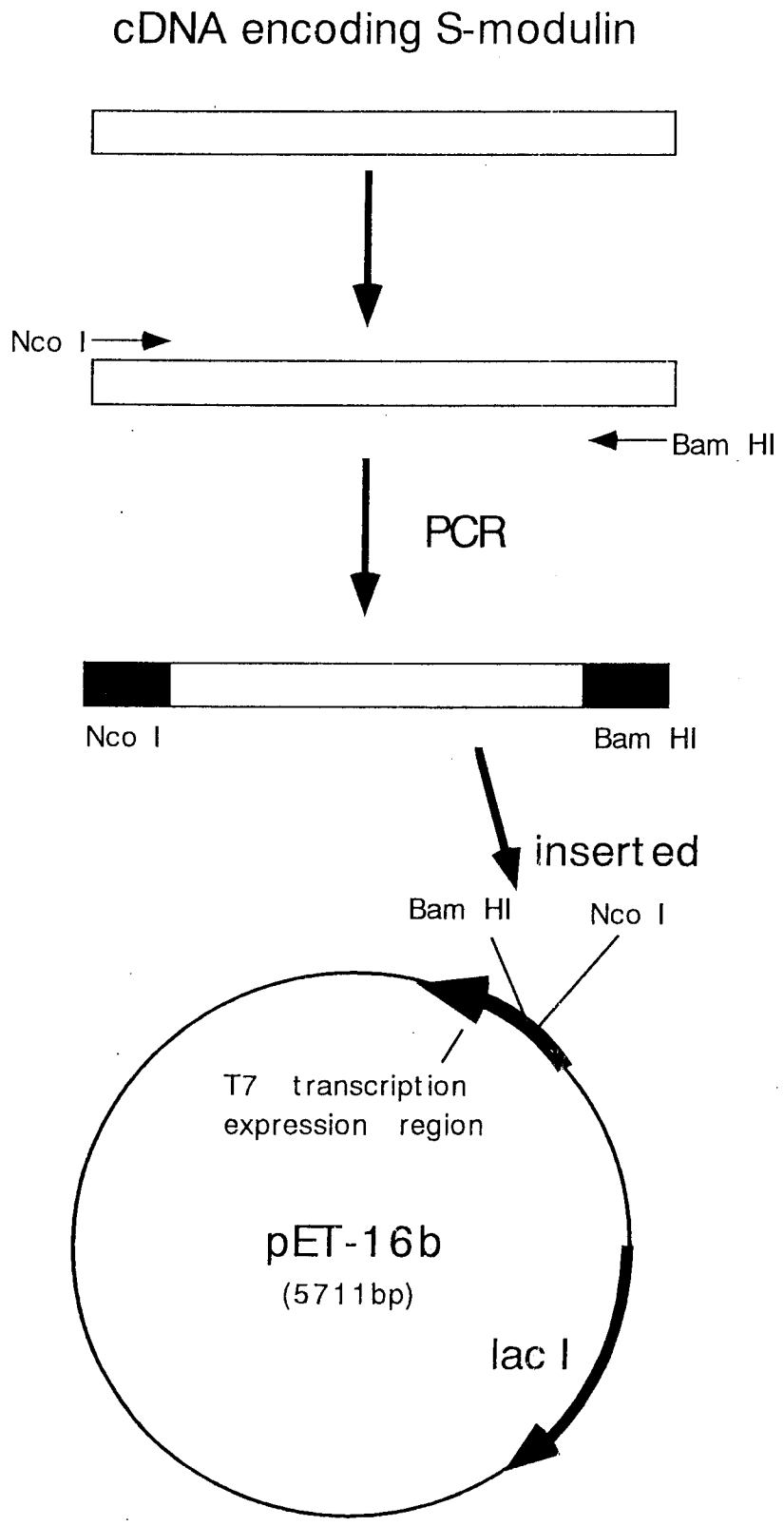

Figure 3-1: The construction of expression vector for S-modulin

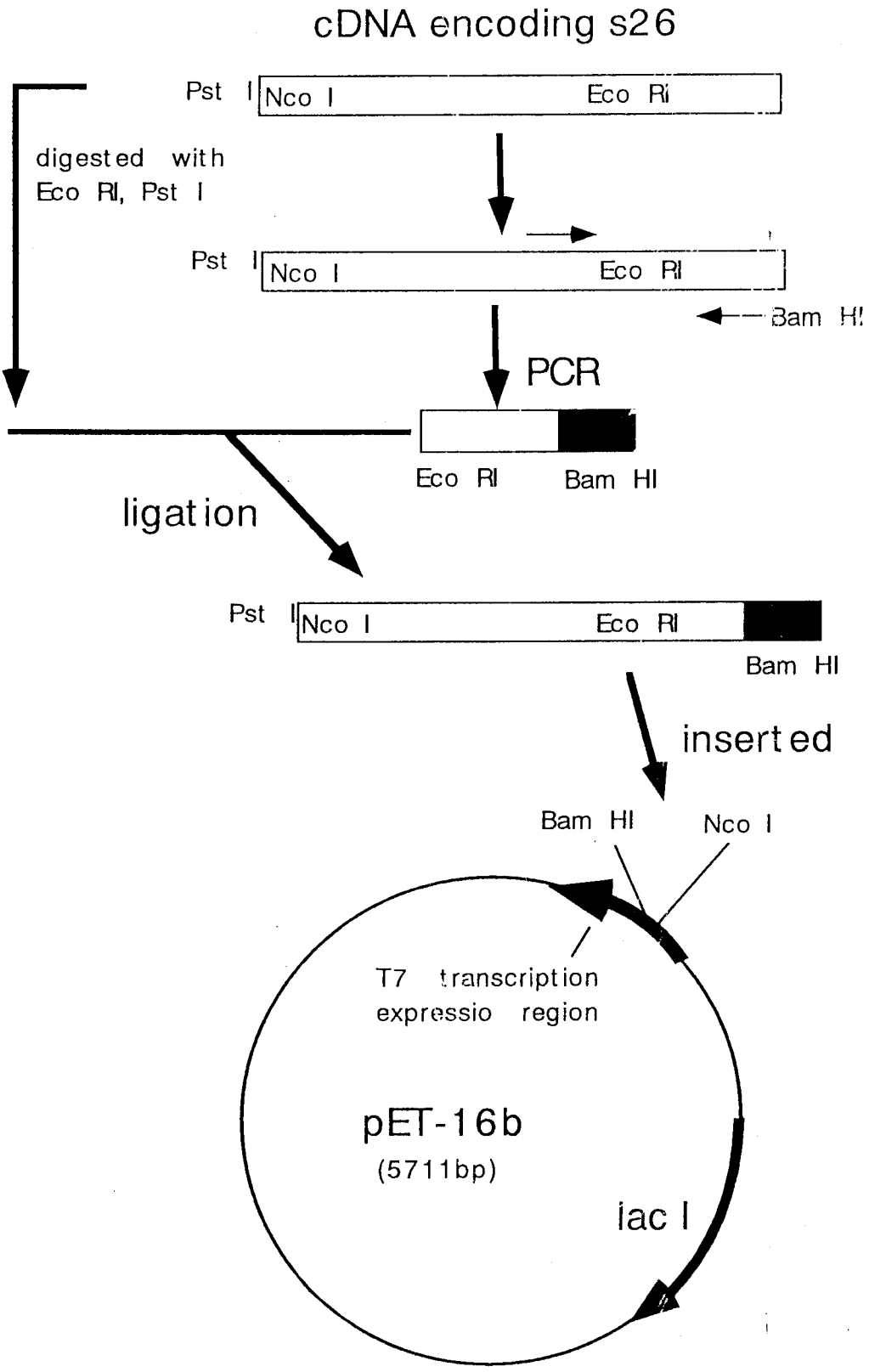

Figure 3-2: The construction of expression vector for s26

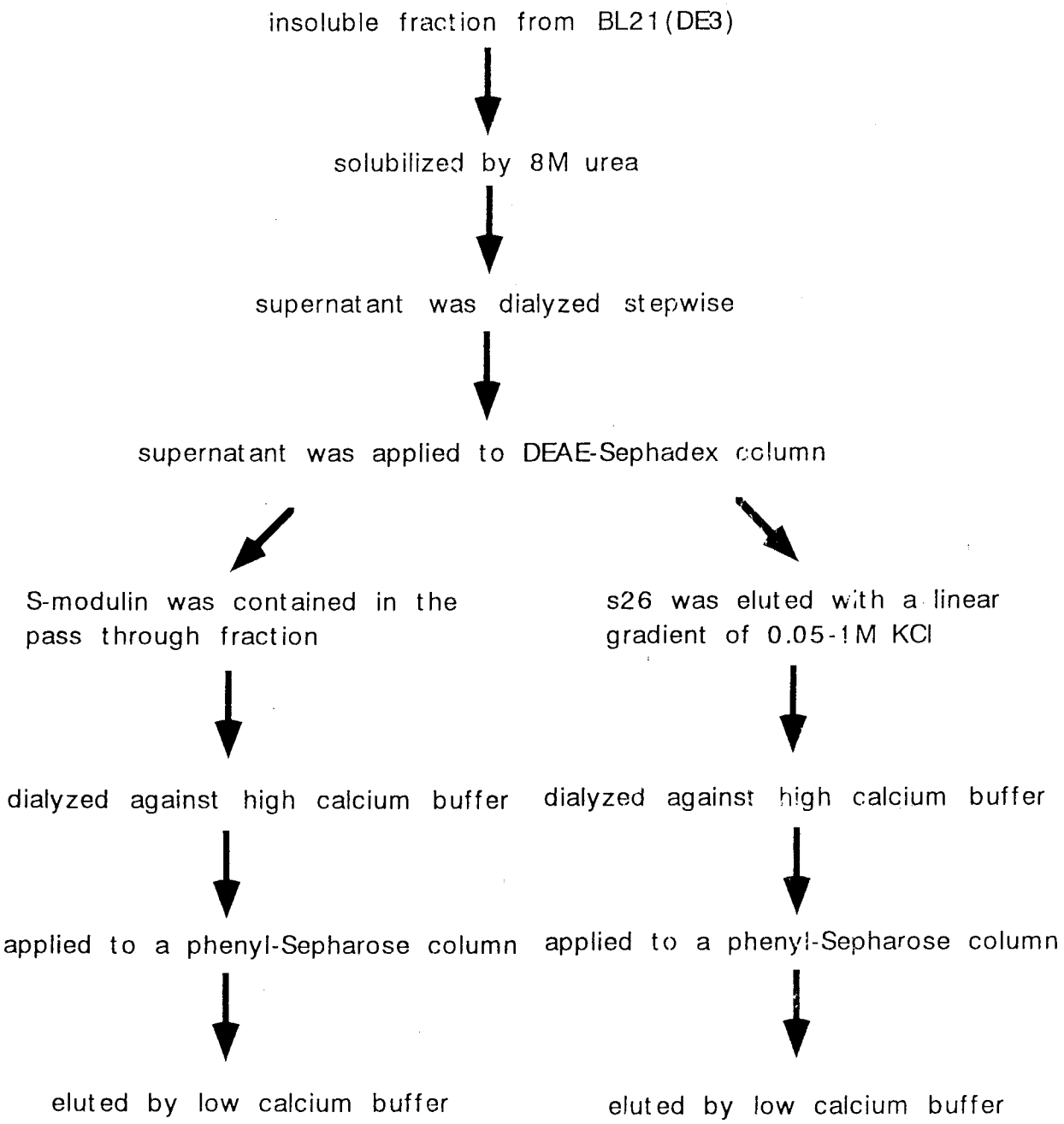

Figure 3-3: Purification of eS-modulin and es26

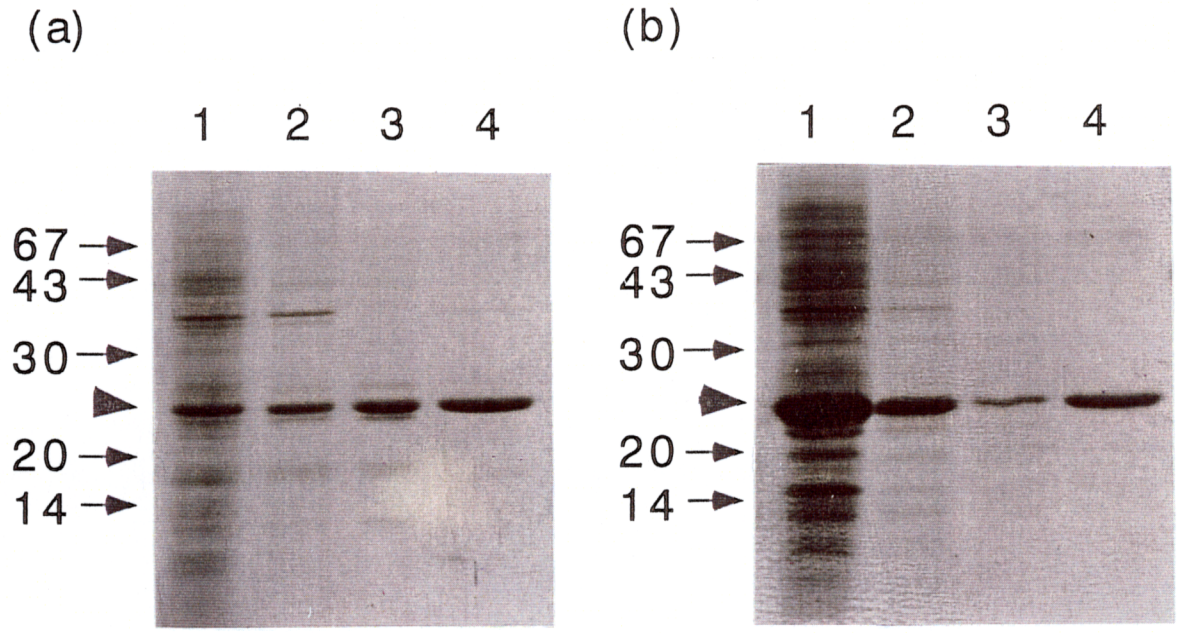

Figure 3-4: Expression and purification of eS-modulin (a) and es26 (b), expressed in BL21(DE3) cells: total protein (lane 1); insoluble fraction (lane 2); and soluble fraction after purification by DEAE-Sephadex (lane 3) and phenyl-Sepharose (lane 4) column chromatographic steps. Arrows indicate mobility of molecular weight markers (kD), and arrowheads the bands of recombinant proteins.

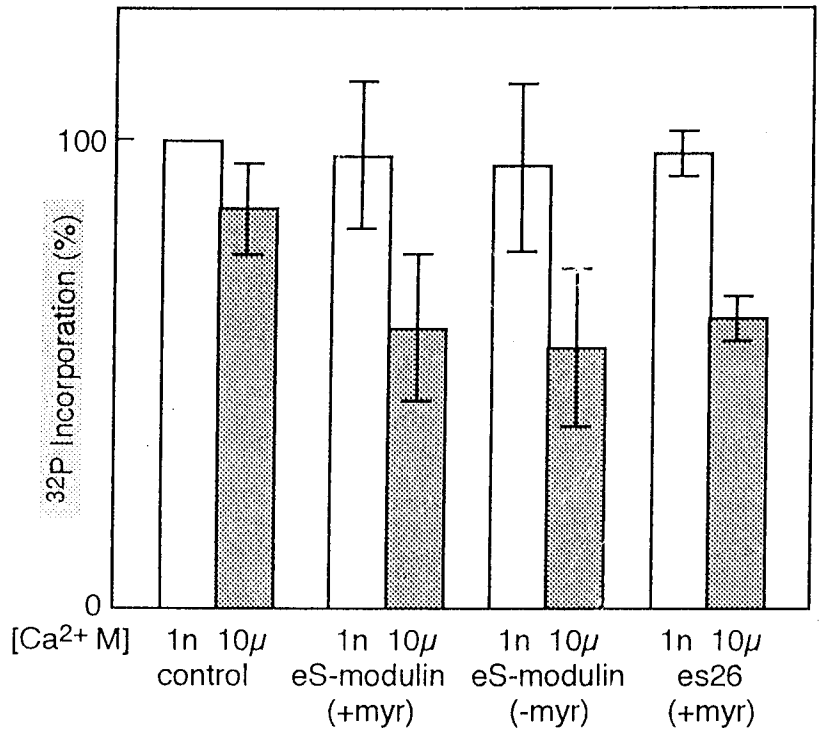

Figure 3-5: ^{32}P-incorporation of rhodopsin in the presence of γ-^{32}P-ATP at low (1 nM; open bars) and high (10 μM; shaded) Ca^{2+} concentrations. Experiments were carried out without recombinant proteins (control), in the presence of 8 μM of myristoylated (+myr) or unmyristoylated (-myr) eS-modulin, or myristoylated (+myr) es26. Bars represent standard deviations from the means of experiments.

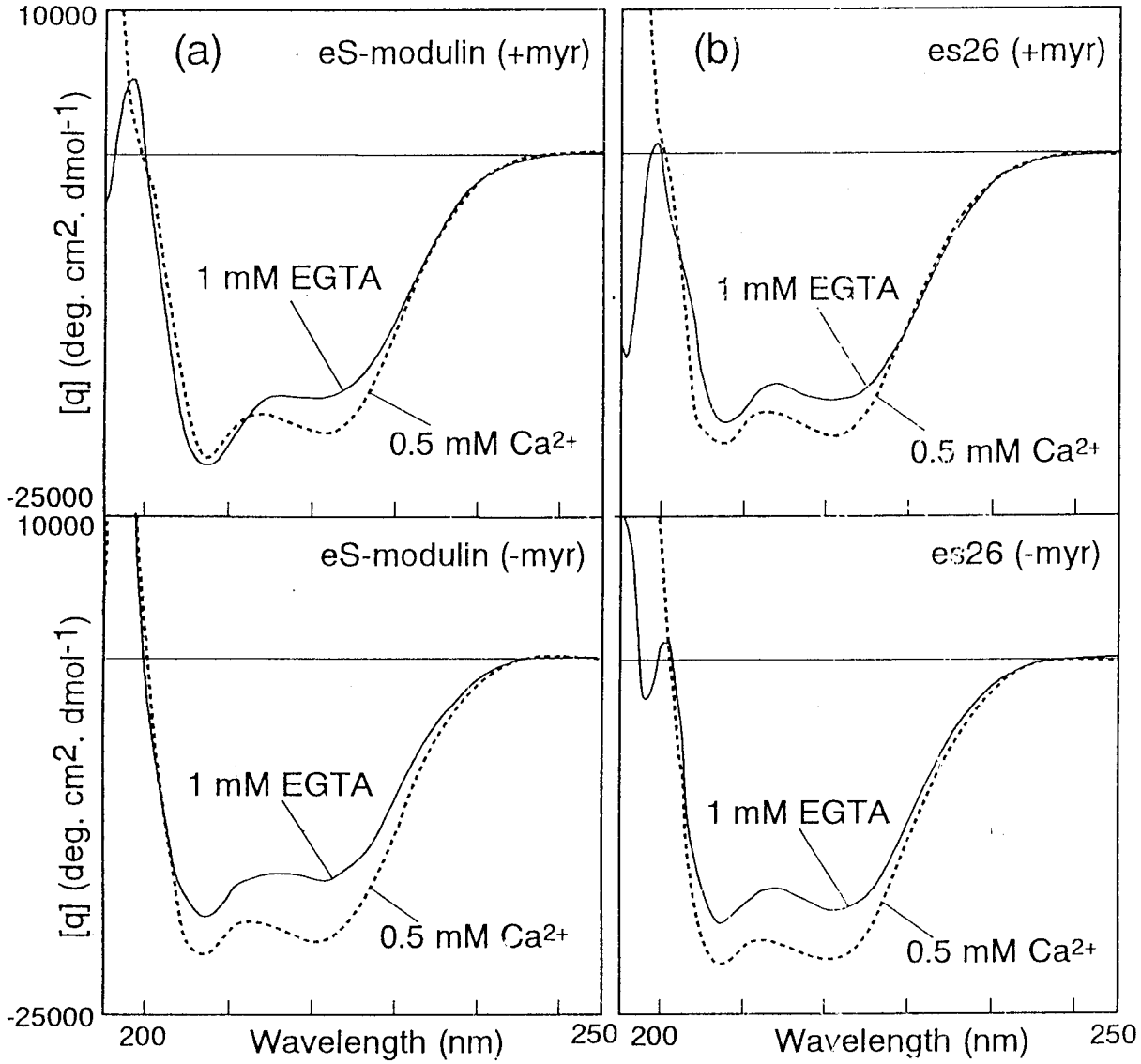

Figure 3-6: CD spectral changes of myristoylated (+myr; upper panels) and unmyristoylated (-myr; lower panels) eS-modulin (a) and es26 (b), in the presence of 1 mM EGTA (solid lines) or 0.5 mM $CaCl_2$ (dashed lines).

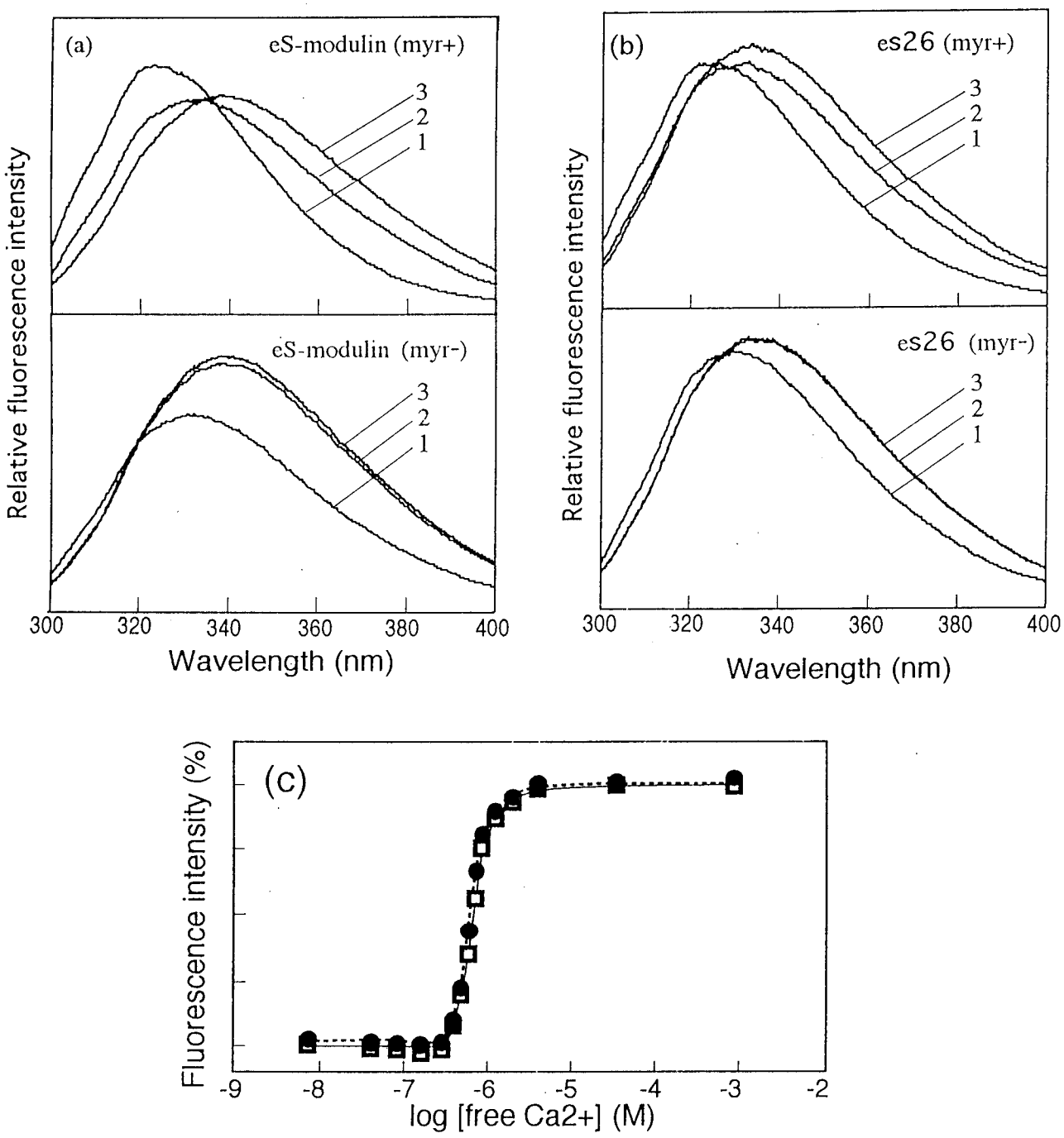

Figure 3-7: Fluorescence emission spectra of myristoylated (+myr; upper panels) and unmyristoylated (-myr; lower panels) eS-modulin (a) and es26 (b), in the presence of 1 nM (curve 1), 0.77 μM (curve 2), or 1 mM (curve 3) free Ca^{2+}. (c) Emission intensity at 370 nm and titration curves for eS-modulin (+myr; open squares and solid line) and for es26 (+myr; closed circles and dashed line).

References

1. Matthews, H.R., Murphy, R.L., Fain, G.L., and Lam, T.D. (1988) Nature 334, 67-69.
2. Nakatani, K. and Yau, K.-W. (1988) Nature 334, 69-71.
3. Kawamura, S. and Murakami, M. (1991) Nature 349, 420-423.
4. Kawamura, S. (1993) Nature 362, 855-857.
5. Haynes, L. and Yau, K.-W. (1985) Nature 317, 61-64.
6. Cobb, W.H., Barkdoll, A.E., and Pugh, E.N. (1985) Nature 317, 64-66.
7. Nathans, J., Thomas,D., and Hogness, D.S. (1986) Science 232, 193-202.
8. Lerea, C.L., Somers, D.E., Hurley, J.B., Klock, I.B., and Bunt-Milam, A.H. (1986) Science 234, 77-80.
9. Hurwitz, R.L., Bunt-Milam, A.H., Change, M.L., and Beavo, J.A. (1985) J. Biol. Chem. 260, 568-573.
10. Baylor, D.A. (1987) Invest. Opthalmol. Visual Sci. 28, 34-49.
11. Normann, R.A. and Werblin, F.S. (1974) J. Gen. Physiol. 63, 37-61.
12. Kawamura, S., Kuwata, O., Yamada, M., Matsuda, S., Hisatomi, O., and Tokunaga, F. (1996) J. Biol. Chem. 271, 21359-21364.
13. Kawamura, S., Hisatomi, O., Kayada, S., Tokunaga, F., and Kuo, C.-H. (1993) J. Biol. Chem. 268,14579-14582.
14. Hisatomi, O., Kayada, S., Aoki, Y., Iwasa, T., and Tokunaga, F. (1994) Vision Res. 34, 3097-3102.
15. Duronio, R.I., Jackson-Machelski, E., Heuckeroth, R.O., Olins, P.O., Devine, C.S., Yonemoto, W., Slice, L.W., Taylor, S.S., and Gordon, J. I. (1990) Proc. Natl. Acad. Sci. USA 87, 1506-1510.

16. Sitaramayya, A. and Margulis, A. (1992) Biochemistry 31, 10652-10656.

17. Tsien, R. and Pozzan, T. (1989) Methods Enzymol. 12, 230-262.

18. Kataoka, M., Mihara, K., and Tokunaga, F. (1993) J. Biochem. 114, 535-540.

19. Ray, S., Zozulya, S., Niemi, G.A., Flaherty, K.M., Brolley, D., Dizhoor, A.M., McKay, D.B., Hurley J., and Stryer L. (1992) Proc. Natl. Acad. Sci. USA 89, 5705-5709.

20. Flaherty, K. M., Zozulya, S., Stryer, L., and McKay, D. B. (1993) Cell 75, 709-716.

21. McCubbin, W. D., Oikawa, K., and Kay, C. M. (1986) FEBS Lett. 195, 17-22.

22. Zozulya, S. and Stryer, L. (1992) Proc. Natl. Acad. Sci. USA 89, 11569-11573.

23. Sanada, K., Kokame, K., Yoshizawa, T., Takao, T., Shimonishi, Y., and Fukada, Y. (1995) J. Biol. Chem. 270, 15459-15462.

24. James, G., and Oleson, E. N. (1990) Biochemistry 29, 2623-2634.

25. Dizhoor, A.M., Chen, C.K., Olshevskaya, E., Sinelnikova, V.V., Phillipov, P., and Hurley, J.B. (1993) Science 259, 829-832.

26. Kawamura, S., Cox, J. A., and Nef, P. (1994) Biochem. Biophys. Res. Commun. 203, 121-127.

27. Calvert, P. D., Klenchin, V. A., and Bownds, M. D. (1995). J. Biol. Chem. 270, 24127-24129.

28. Senin, I.I., Zargarov, A.A., Alekseev, A.M., Gorodovikova, E.N., Lipkin, V.M., and Philippov, P.P. (1995) FEBS Lett. 376, 87-90.

29. Chen, C.-K., Inglese, J., Lefkowitz, R. B., and Hurley, J. B. (1995). J. Biol. Chem. 270, 18060-18066.

30. Hughes, R.E., Brzovic, P.S., Klevit, R.E., and Hurley, J.B. (1995) Biochemistry 34, 11410-11416.

Chapter 4

The Role of S-modulin Carboxyl-Terminal Charges on its Membrane Affinity and Inhibition of Rhodopsin Phosphorylation

Introduction

In the dark-adapted photoreceptors of vertebrates, cGMP-gated cation channels are opened and Ca^{2+} flows into the cell (1, 2). Intracellular Ca^{2+} is continuously pumped out by a Na^{+}-K^{+}/Ca^{2+} exchanger in the outer segment (3, 4). Light initiates the phototransduction cascade, closes the cation channels, and blocks the Ca^{2+} influx. The result is a cytoplasmic Ca^{2+} concentration decrease in the light-adapted state. This decrease of Ca^{2+} concentration is the underlying mechanism of light adaptation of the vertebrate photoreceptor (5, 6). A frog photoreceptor Ca^{2+}-binding protein, S-modulin, and its bovine homologue, recoverin (7), inhibit the phosphorylation of light-activated rhodopsin at high Ca^{2+} concentration, but do not interfere at low Ca^{2+} concentration (8, 9). As phosphorylation of the rhodopsin carboxyl-terminus is thought to be the shut off mechanism for the activation of transducin (10, 11), S-modulin and recoverin contribute to increased light-sensitivity in the dark-adapted state (high Ca^{2+} concentration). These Ca^{2+}-binding proteins associate with rod outer segment (ROS) membrane at high but not at low Ca^{2+} concentrations, a process involving N-terminal acylation (N-myristoylation): the "Ca^{2+}-myristoyl switch" (12, 13).

The basic signal transduction pathway is thought to be similar for rods and cones (14-18) but there are some differences. Rods are more sensitive than cones, and the light response of cones is faster and is terminated more rapidly than that of rods (19). We have found another Ca^{2+}-binding protein, s26, in frog retina which is localized to cone photoreceptor cells, suggesting that S-modulin and s26 regulate the phosphorylation of rhodopsin and cone pigment, respectively (20). The Ca^{2+}-dissociation constants of S-modulin and s26 show only a small difference (21).

In the this section, I first describe the membrane affinities of recombinant

S-modulin and s26 with or without N-myristoylation, demonstrating that N-myristoylation is important for membrane-binding and that S-modulin has a higher affinity for ROS membrane than s26. Second, I describe the membrane affinities of recombinant proteins and the efficiency of their ability to inhibit rhodopsin phosphorylation, which is shown to coincide with an increase in the number of C-terminal positive charges.

Experimental Procedures

Construction of expression vectors for chimeric proteins and site-directed mutants— I tried to express chimeric proteins and site-directed mutants shown in figure 4-1. cDNA fragments were exchanged between NcoI and EcoRI recognition sites of plasmid vectors, pET-Smd and pET-s26 (containing S-modulin and s26 coding regions, respectively) (21). The resulting plasmids (pET-Smd/173/s26 and pET-s26/173/Smd) were used as expression vectors for chimeric S-modulins and s26, respectively.

S-modulin cDNA cloned into a plasmid vector (9) was used as the template for polymerase chain reaction to generate site-directed mutants. Oligonucleotide primers 5'-GCGTCGACTCGAGCTAGTGTTGTTGCTCTTGTAGCTGGTCCTGGACTTGTTGAGG TTCGT-3', and 5'-GCGTCGACTCGAGCTAGTGTTTTTTCTGTTTTAGCTTGTTCTTGAC TTTTTGAGGTTCGT-3' were made to generate S-modulin mutants, Smd/del+ (K192/194/196/198/200/201Q, lysine residues at 192, 194, 196, 198, 200 and 201 of S-modulin were replaced with glutamine) and Smd/del- (D195N/E199Q, Asp195 and Glu199 were replaced with Asn and Gln, respectively). Using SMD-NTF as an external primer (21), mutant cDNAs were amplified and inserted between NcoI and XhoI sites of

a pET-16b (Novagen) plasmid vector (forming vectors pET-Smd/del+ and pET-Smd/del-).

Expression and purification of recombinant proteins — The procedures of expression and purification of the recombinant proteins have been described in detail by Hisatomi et al (21). Briefly, the expression vectors, pET-Smd, pET-s26, pET-s26/173/Smd, pET-Smd/173/s26, pET-Smd/del+ and pET-Smd/del- were transfected to *E. coli*, BL21DE3 (Novagen) with (+myr) or without (-myr) pBB131, an expression vector of *N*-myristoyl transferase. The recombinant proteins were expressed by the addition of 1 mM isopropyl-β-*D*-thiogalactopyranoside, solubilized with 8 M urea buffer, refolded by three steps of dialysis, and applied to a DEAE-Sephadex column. S-modulin, Smd/173/s26, Smd/del+ and Smd/del- were contained in the pass-through fraction, and s26 and s26/173/Smd were eluted with 400 mM KCl. The recombinant proteins in the high Ca^{2+} buffer were then applied to a phenyl-Sepharose column and eluted by decreasing the Ca^{2+} concentration.

Preparation of frog rod outer segment membranes— Retinas were dissected from bullfrogs, *Rana catesbeiana* (about 10 cm in length). ROS membranes were isolated by flotation on 45% sucrose in gluconate buffer (40 mM K-gluconate, 2.5 mM KCl, 2 mM $MgCl_2$, 1 mM DTT, 1 mM EGTA, 10 mM HEPES, pH 7.5), and washed twice with gluconate buffer, and then with gluconate buffer containing 4 M urea to eliminate (strip away) endogenous S-modulin, s26 and other peripheral proteins, and used (as "urea-stripped ROS membranes") for membrane binding experiments. For the phosphorylation assay, ROS membranes were isolated in phosphorylation buffer (115 mM K-gluconate, 2.5 mM KCl, 2 mM $MgCl_2$, 1 mM DTT, 1 mM EGTA, 10 mM HEPES, pH 7.5) in complete darkness with the aid of an infrared converter and washed three

times with the same buffer to eliminate endogenous S-modulin, s26 and ATP.

Ca^{2+}-dependent membrane association of recombinant proteins— Membrane binding properties of the recombinant proteins were investigated according to the method of Kawamura et al. (shown in Fig. 4-2 Ref: 22), using plastic tubes siliconized to prevent non-specific binding. ROS membranes containing 6 nmole rhodopsin were mixed with 0.5 ml gluconate buffer, containing 1% bovine serum albumin to block non-specific binding sites. After washing twice by centrifugation (37,000 x g for 5 min at 4 °C) with 1 ml gluconate buffer containing 1 mM free Ca^{2+} (adjusted by Ca^{2+}/EGTA buffer) and from 0 to 500 mM NaCl (Ca^{2+}-NaCl gluconate buffer), the ROS membranes were re-suspended in 20 μl Ca^{2+}-NaCl gluconate buffer containing recombinant proteins (120 pmol). The mixtures were then incubated at room temperature for 30 min and then centrifuged (37,000 x g for 5 min at 4 °C) to obtain the recombinant proteins that did not associate with the membranes even at the high (1 mM) Ca^{2+} concentration. Extraction was repeated once to minimize the loss of unbound proteins. The resulting two soluble fractions (high Ca^{2+} extract) were mixed and analyzed by SDS-PAGE. The membrane fractions were then suspended in 20 μl gluconate buffer containing 10 mM EGTA and from 0 to 500 mM NaCl (EGTA-NaCl gluconate buffer), and centrifuged to extract proteins liberated from the membrane by decreasing the Ca^{2+} concentration. The extraction was repeated and the resulting two soluble fractions (low Ca^{2+} extract) and membrane fractions were analyzed by SDS-PAGE. The integrated densities of Coomassie Brilliant Blue (CBB) stained bands of the recombinant proteins were quantified by a two dimensional densitometer (pdi. The Discovery Series).

Rhodopsin phosphorylation— Rhodopsin phosphorylation was measured by the method of Kawamura (8) and Sanada et al (23) (shown in Fig. 4-6). Briefly, the reaction

was carried out in 25μl of the mixture, containing rhodopsin (final concentration 10 μM) and recombinant proteins (1 μM) in phosphorylation buffer. Free calcium concentration in the mixture was adjusted by adding 1M $CaCl_2$ solution. The reaction mixtures were exposed to light for 2 min, and the phosphorylation reactions were initiated by adding ATP (0.1 mM, final concentration), [γ-^{32}P] ATP (0.25 μM, 168 TBq/mmol) and GTP (0.5 mM). After incubation at room temperature for 2 min in light, the reaction was terminated by an addition of 150 μl 10% trichloroacetic acid. The reaction mixtures were then centrifuged (10,000 x g) for 5 min, and the precipitates were washed with 500 μl of phosphorylation buffer and applied to SDS-PAGE. The incorporation of ^{32}P into rhodopsin was evaluated with an image analyzer (bas 2000 Fuji Film).

Results

Membrane association of recombinant expression products —To investigate the membrane-binding properties of S-modulin and s26, we carried out extraction experiments using urea-stripped ROS membranes and recombinant proteins as described by Kawamura et al (22). The recombinant proteins, either myristoylated (eS-modulin (+myr) and es26 (+myr)) or unmyristoylated (eS-modulin (-myr) and es26 (-myr)) (21), were mixed with urea-stripped ROS membranes at high Ca^{2+} concentration. Soluble fractions (high Ca^{2+} extracts) containing proteins that did not bind to ROS membrane even at high Ca^{2+} concentration were stored. Membrane fractions were re-suspended with low calcium (10mM EGTA) buffer, and centrifuged to isolate the supernatant (low Ca^{2+} extracts) containing proteins that were liberated from the membrane by lowering calcium concentration. The high and low Ca^{2+} extracts and

membrane fractions were analyzed by SDS-PAGE. The amount of recombinant proteins remaining in the final membrane fractions was less than 5% (data not shown), indicating that these recombinant proteins exhibit virtually no binding to the membrane at low Ca^{2+} concentration. The ratio of membrane-bound protein (low Ca^{2+} extract)/(high Ca^{2+} extract + low Ca^{2+} extract) was estimated to be 54.7% for eS-modulin (+myr), 36.0 % for es26 (+myr), 13.7% for eS-modulin (-myr) and 4.6% for es26 (-myr) (Fig. 4-3 unshaded bars). These results indicate that (i) the N-terminal myristoylation is very important for the membrane association of both S-modulin and s26; and (ii) the membrane affinity of eS-modulin is greater than that of es26. In our Western blot analysis, a similar difference of membrane affinity was observed between native S-modulin and s26 in frog retina (data not shown). The latter difference in membrane affinity also seems to be due to differences in the protein moiety, because even unmyrstoylated eS-modulin (-myr) showed a higher membrane affinity than es26 (-myr).

The same extraction experiments were carried out with boiled ROS membrane (Fig. 4 shaded bars), which did not affected the binding ratio.

Electrostatic interaction to Ca^{2+}-dependent membrane association —To reduce electrostatic interaction, the same extraction experiments were carried out in the presence of various concentrations of NaCl. Figure 4-4 shows that the membrane affinity of eS-modulin was reduced to that of es26 levels by increasing the NaCl concentration, so it is concluded that S-modulin binds to the ROS membrane by electrostatic interactions in the protein moiety as well as by hydrophobic interaction of the N-terminal myristoyl group.

Membrane-association of chimeric and mutant proteins— Two myristoylated chimeric recombinants, es26/173/Smd (+myr) and eSmd/173/s26 (+myr), were made with the N-terminal 173 amino acids from s26 and S-modulin but with the remaining C-terminal residues swapped: that is from S-modulin and s26 sequences, respectively. The ratios of membrane bound protein were 64.0 % for es26/173/Smd (+myr) and 40.5 % for eSmd/173/s26 (+myr) at 0 mM NaCl (Fig. 4-5). suggesting strongly that the carboxyl terminus of S-modulin enhances ROS membrane affinity.

Two site-directed mutants of myristoylated S-modulin were also isolated, eSmd/del+ (+myr) and eSmd/del- (+myr), in which positively and negatively charged residues near the C-terminal were replaced with neutral residues (K192/194/106/198/200/201Q and D195N/E199Q), respectively. The ratio of membrane bound protein was 29.6 % for eSmd/del+ (+myr) and 74.3 % for eSmd/del- (+myr) (Fig. 4-5), indicating that the C-terminal charges of S-modulin are important for membrane binding.

Inhibition of rhodopsin phosphorylation by recombinant proteins — The present study has shown that the Ca^{2+}-binding form of S-modulin has a higher membrane affinity than that of s26, and that this difference is due to charges at the carboxyl terminus (Fig. 4-6). Does this difference of membrane affinity affect the efficiency of rhodopsin phosphorylation? To answer this question, phosphorylation of rhodopsin was examined in the presence of recombinant proteins eS-modulin (+myr), s26 (+myr), s26/173/Smd (+myr), Smd/173/s26 (+myr), eSmd/del+ (+myr) and eSmd/del- (+myr) (Fig. 4-7). All of them inhibited rhodopsin phosphorylation at high (0.1 mM) Ca^{2+} concentration, but there were certain differences in inhibitory efficiency. The recombinant proteins with high membrane affinity, eS-modulin (+myr), es26/173/Smd (+myr) and eSmd/del- (+myr), inhibit rhodopsin phosphorylation more efficiently than

proteins with low membrane affinity, such as es26 (+myr), eSmd/173/s26 (+myr) and eSmd/del+ (+myr). These results indicate that the C-terminal positive charges increase the inhibitory effect on rhodopsin phosphorylation.

Discussion

The mechanism of membrane association — Our results suggest that S-modulin binds to the ROS membrane not only by hydrophobic interaction with the N-terminal myristoyl group but also by electrostatic interaction with the C-terminal charges. It has been reported that S-modulin also binds to ROS membrane lipid extracted with chloroform-methanol (24), so it is likely that these proteins bind to the membrane lipid rather than membrane proteins. Our result shown in figure 4 (the ratio of membrane bound protein was not affected by boiling ROS membranes) also supports this suggestion.

Although the structure of myristoylated bovine S-modulin (recoverin) is determined by using NMR techniques (25), there was no description about the structure of carboxyl terminus. A part of C-terminal structure (except for residues 199-202) is determined in the unmyristoylated crystal bovine S-modulin with one Ca^{2+} (Fig. 4-8 Ref 26). In this structure, C-terminal positive charges exist in the protein surface and face to various directions. Though the strucrure of S-modulin bound to the ROS membrane was unknown, in order to bind to the membrane effectively, C-terminal positive charges shoud be arranged in the same direction.

I propose a model of membrane-binding forms of S-modulin (Fig. 4-9 A) and s26 (Fig. 4-9 B) by modifying the model proposed for bovine S-modulin (13). This model

can explain the difference in membrane-binding properties between S-modulin and s26. In the Ca^{2+}-binding forms of S-modulin and s26, the N-terminal acyl groups will partition into the phospholipid bilayer, and C-terminal positive charges may bind to the negatively charged lipid head groups. Since the C-terminus of S-modulin has more positively charged amino acids than s26 (9, 20), ROS membrane affinity with S-modulin is higher than that for s26.

Physiological implications of membrane binding properties— There are two groups of these photoreceptor Ca^{2+}-binding proteins (20), one includes S-modulin and recoverin, the other includes s26 and visinin (a cone-specific Ca^{2+}-binding protein found in chicken retina; Ref 27). Bovine, human, and mouse recoverin have 4-6 positively charged residues at their C-terminus (7, 28, 29), whereas visinin has only two (Fig. 4-10). The C-termini of Ca^{2+}-binding proteins belonging to the S-modulin group (rod type proteins) were expected to have more positive charges at physiological pH than those belonging to the s26 group (cone type proteins). Therefore, the rod type proteins may bind to the photoreceptor membrane more tightly and inhibit the phosphorylation of visual pigments more efficiently than the cone type. It has been reported that the phosphorylation of light-activated rhodopsin is required for normal shutoff of the electrophysiological response (11), so the difference in membrane affinities between S-modulin and s26 may explain, at least partly, the more rapid recovery of the photoresponse in cones than in rods.

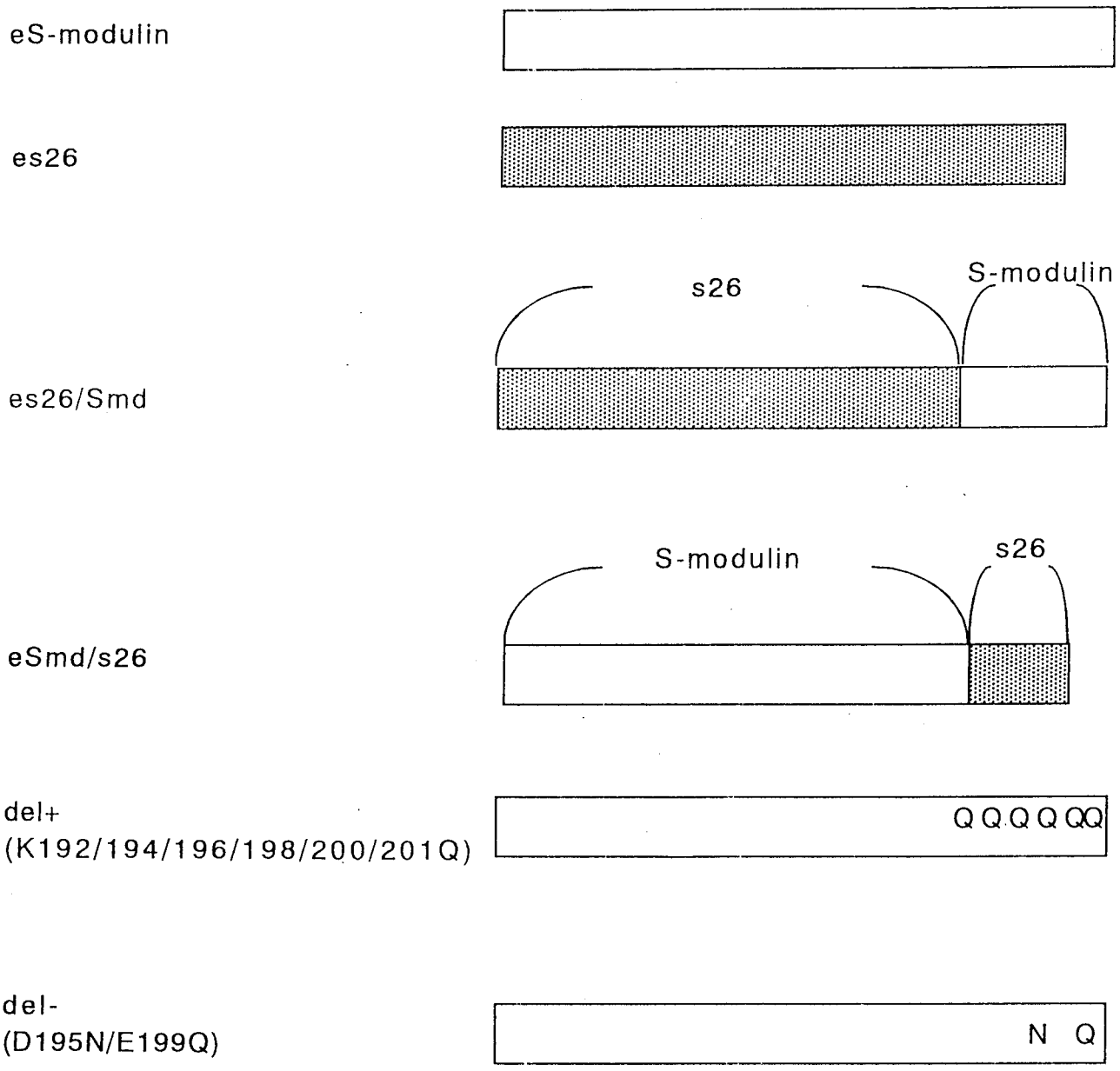

Figure 4-1: A schematic drawing of the recombinant proteins in chapter 4

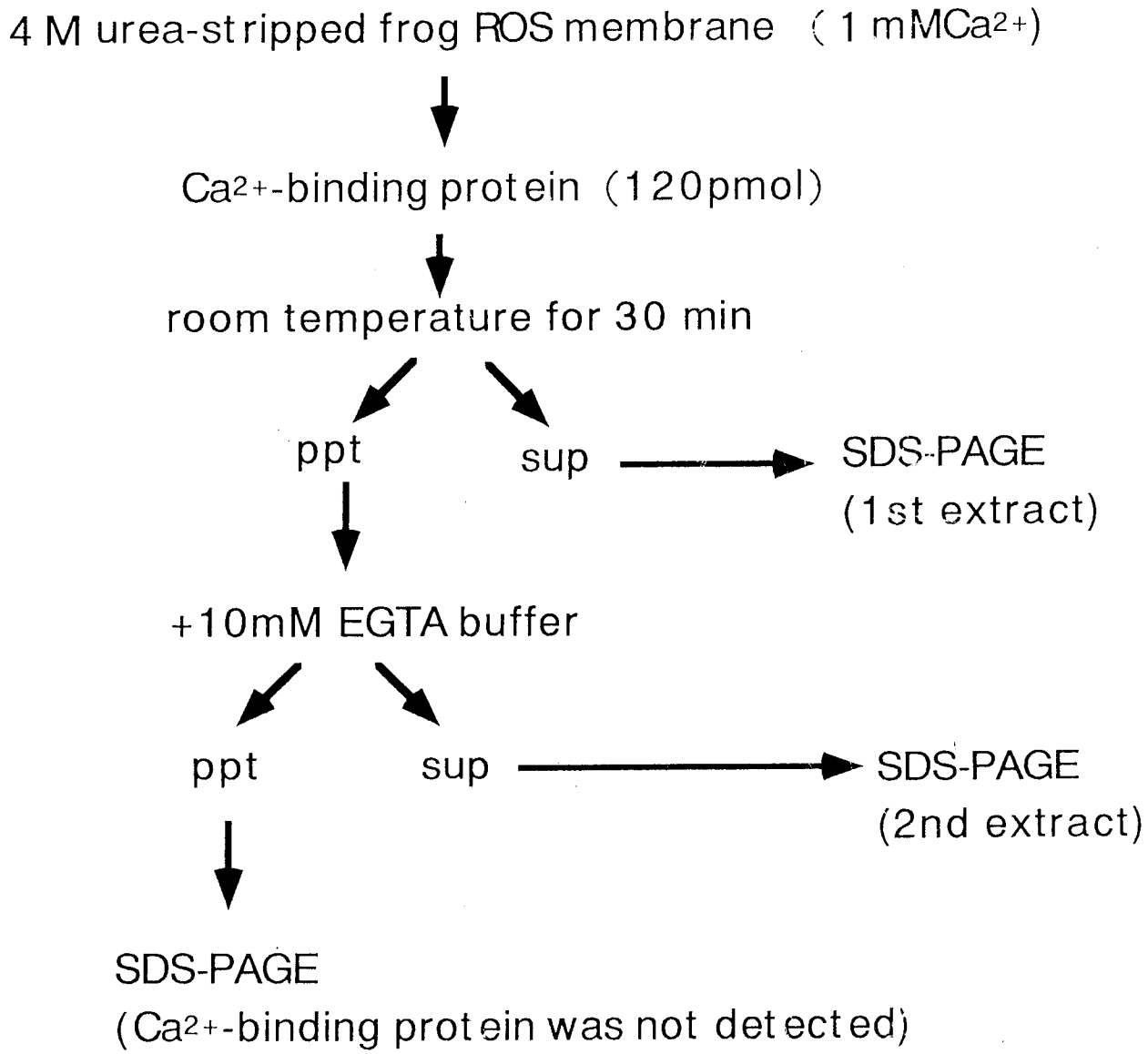

The ratio of membrane bound protein

=2nd extract/(1st extract+2nd extract)

Figure 4-2: A method to investigate membrane-binding properties of recombinant proteins

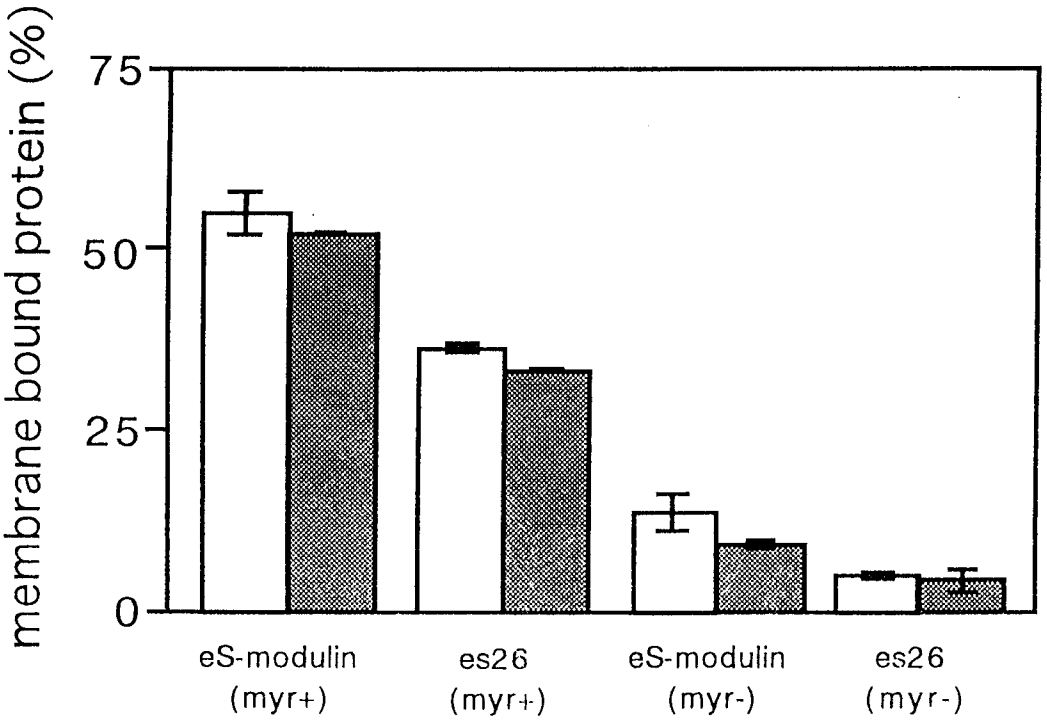

Figure 4-3: Membrane-Binding Properties of S-modulin and s26. Binding of eS-modulin (+myr), es26 (+myr), eS-modulin (-myr), and es26 (-myr) to urea-stripped (open bars) and boiled (shaded bars) ROS membranes, quantified by densitometric analysis of CBB-stained SDS-PAGE bands . Bars represent standard deviations (n = 2).

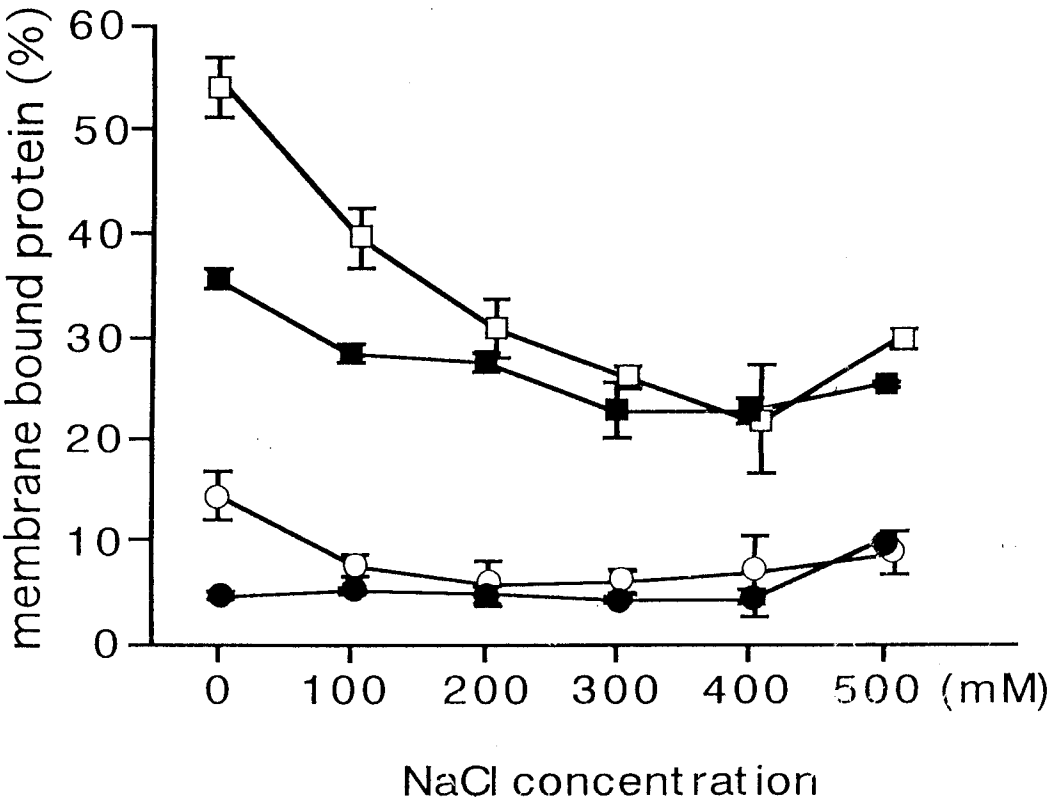

Figure 4-4: NaCl Effects on Membrane association. Binding ratios of eS-modulin (+myr), es26 (+myr), eS-modulin (-myr), and es26 (-myr) to urea-stripped ROS membranes plotted against NaCl concentration. □ : eS-modulin (+myr), ■: es26 (+myr), ○: eS-modulin (-myr), ● : es26 (-myr). Bars represent standard deviations (n = 2).

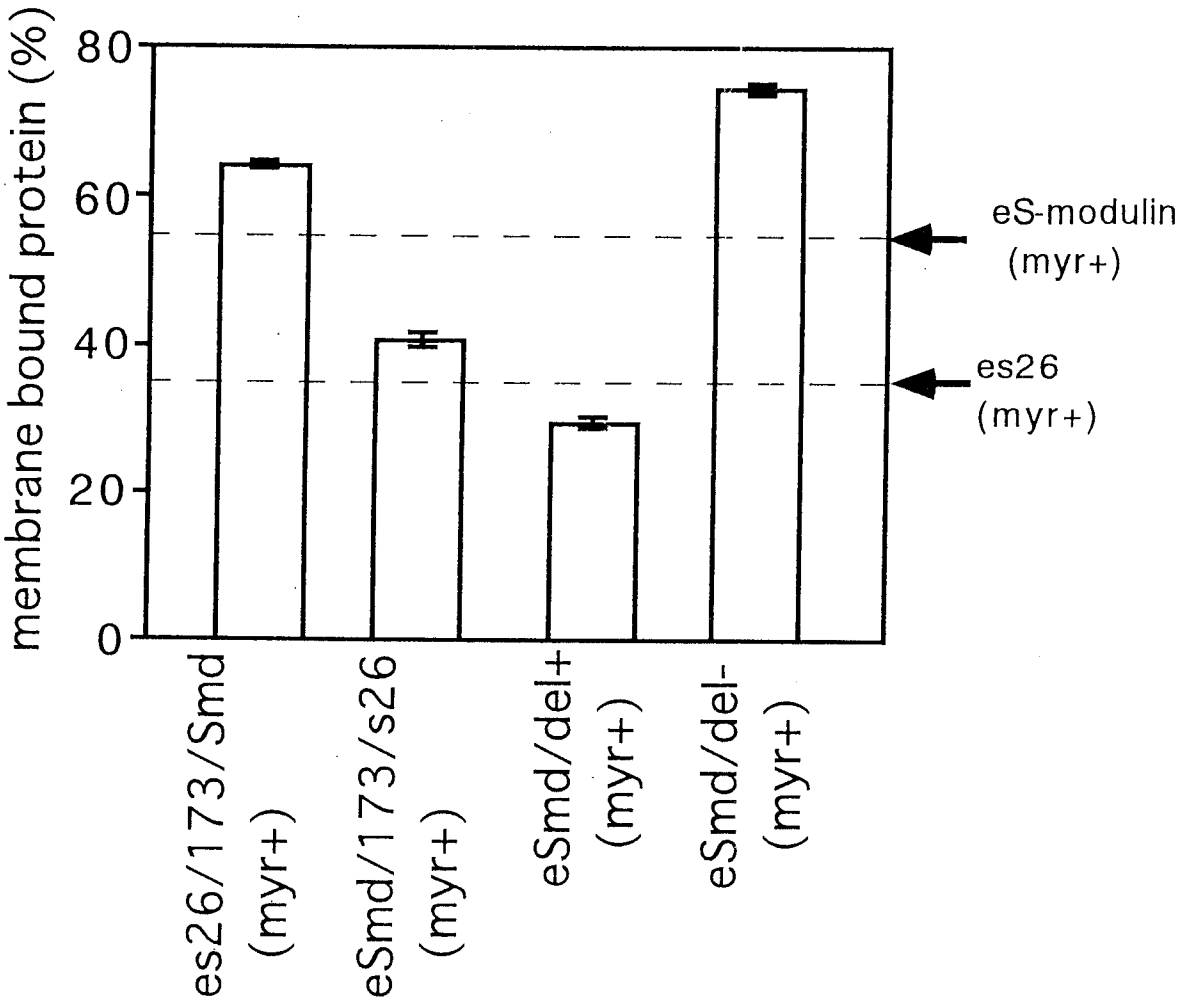

Figure 4-5: Membrane-Binding Properties of Chimeric and Mutant Proteins. Binding of es26/173/Smd (myr+), eSmd/173/s26 (myr+), eSmd/del+ (myr+) and eSmd/del- (myr+) to urea-stripped ROS membranes at 0 mM NaCl concentration. Arrows and dashed lines indicate the membrane bound protein ratios of eS-modulin (myr+) and es26 (myr+). Bars represent standard deviations (n = 2).

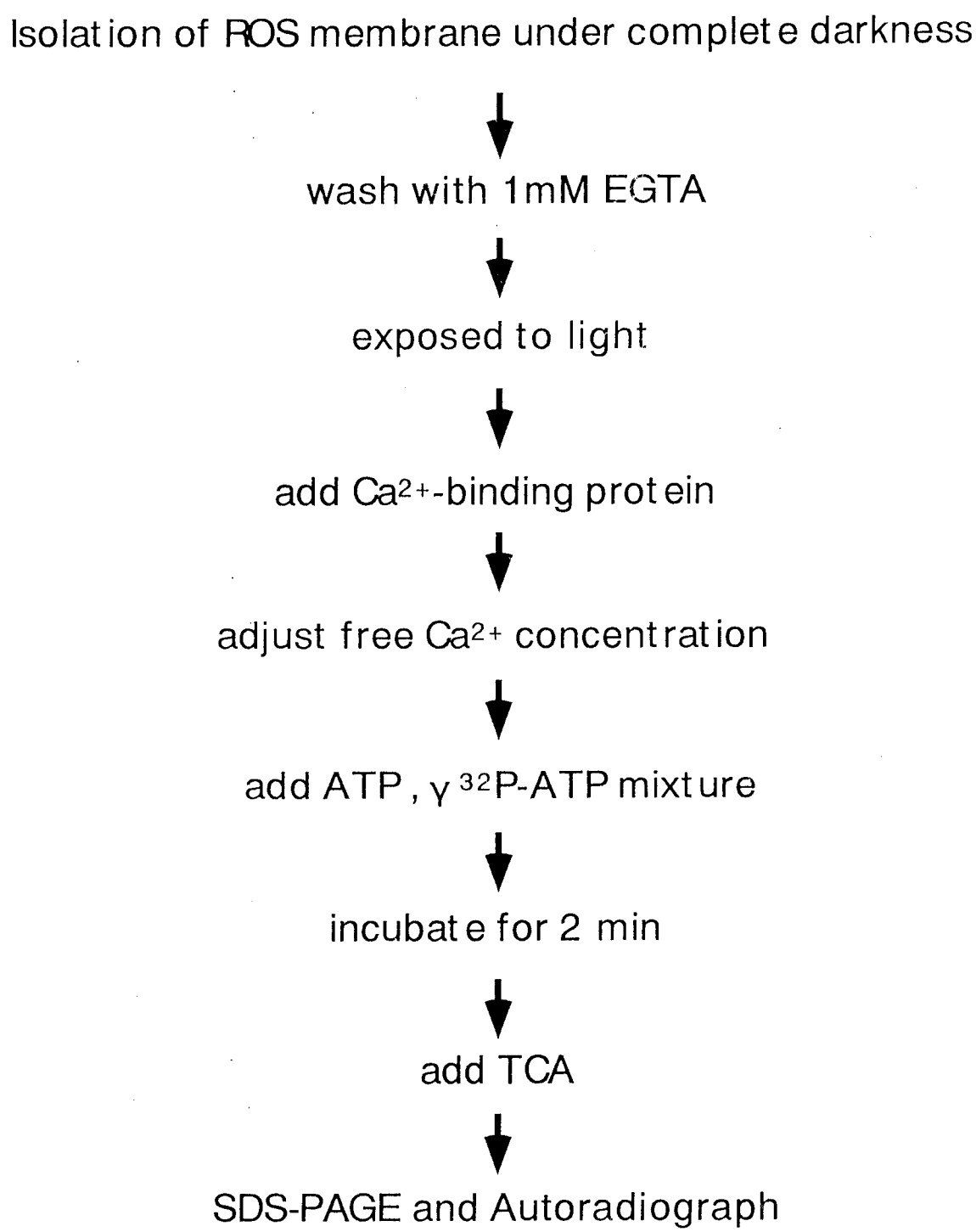

Figure 4-6: A method for measurement of the rhodopsin phosphorylation. The final concentration of rhodopsin and Ca^{2+}-binding protein are 10μM and 1μM, respectively

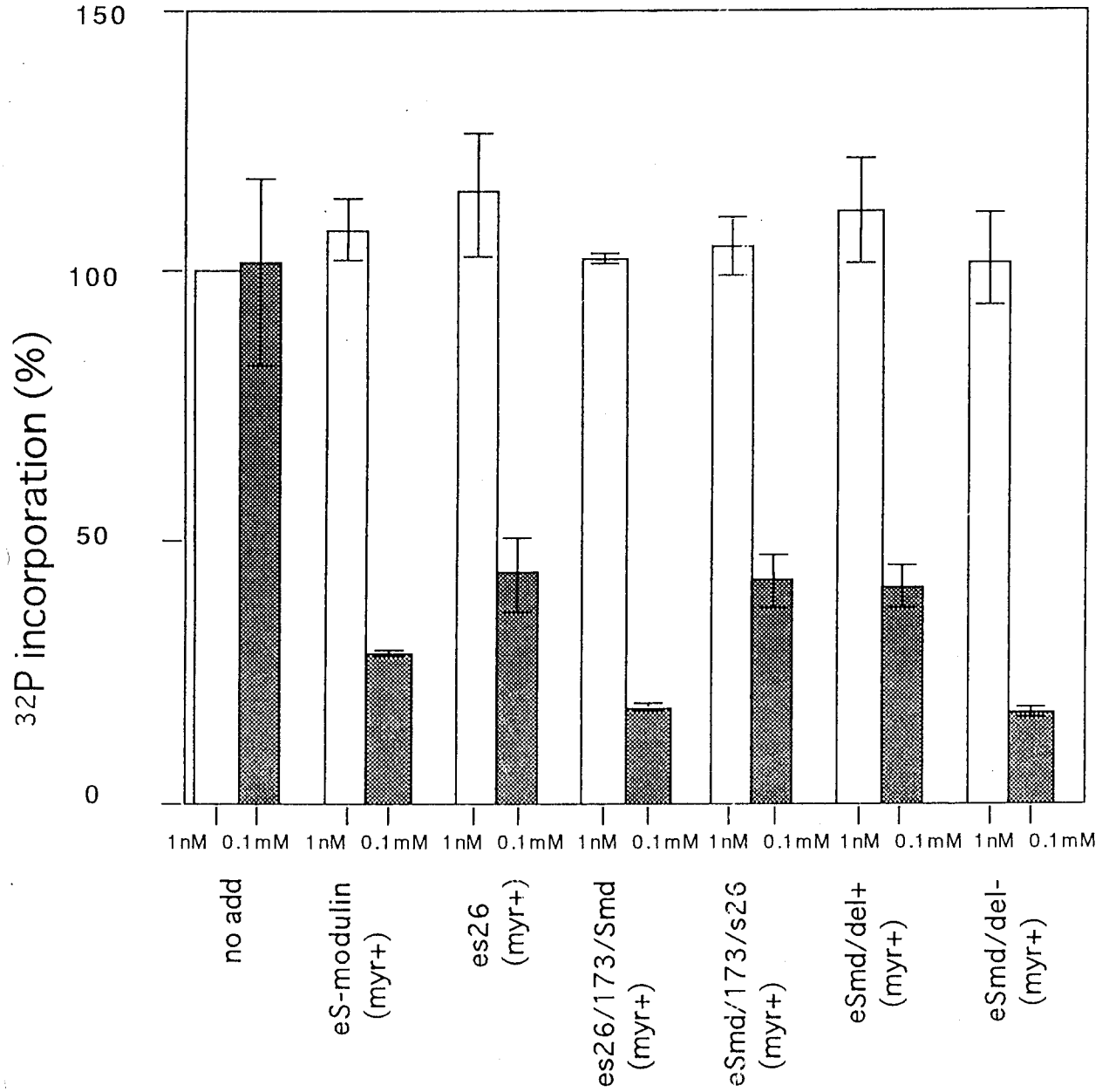

Figure 4-7: Inhibition of Rhodopsin Phosphorylation. ^{32}P incorporation of rhodopsin in the presence of [γ-^{32}P] ATP at low (1 nM, open bars) and high (0.1 mM, shaded bars) Ca^{2+} concentrations. Experiments were carried out without recombinant proteins (control), or in the presence of 1μM recombinant proteins. Bars represent standard deviation (n = 2).

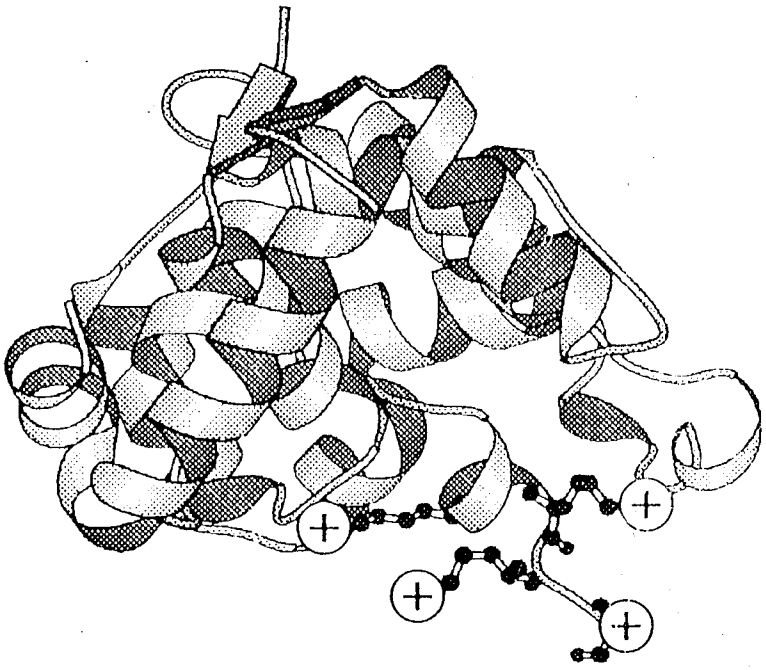

Figure 4-8: A crystal stracture of unmiristoylated bovine S-modulin with one Ca^{2+}. Lysine residues at carboxyl terminus (192-198) were shown in ball and stick model. + indicate positive charges. This figure is made by using MOLSCRIPT (a program to produce both detailed and schematic plots of protein structure Ref 30)

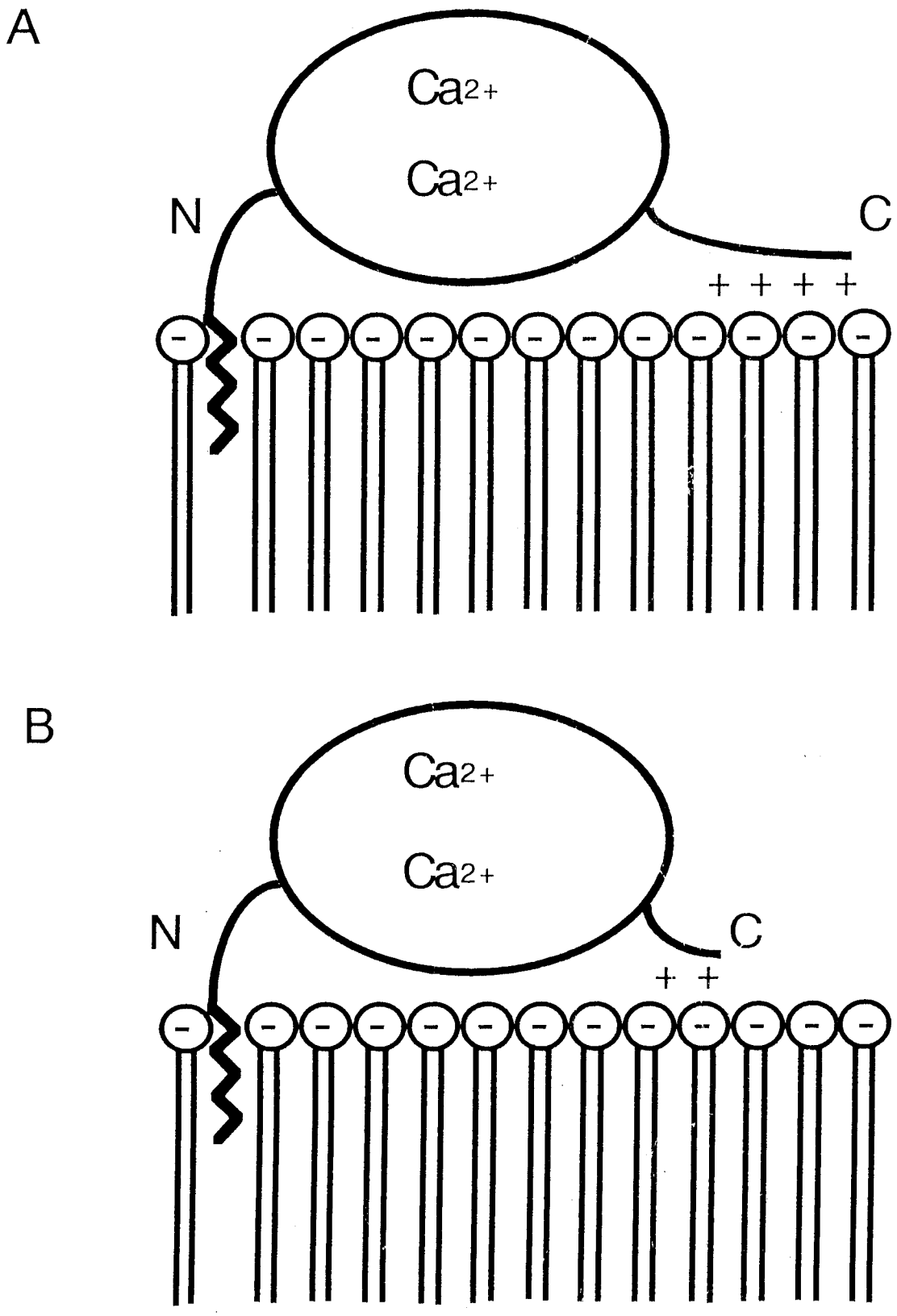

Figure 4-9: A Model for Membrane Association of S-modulin and s26. (A) and (B) indicate membrane-bound myristoylated S-modulin and s26, respectively.

+ and - represent, respectively, protein C-terminal positive charges and negative charges on lipid head groups.

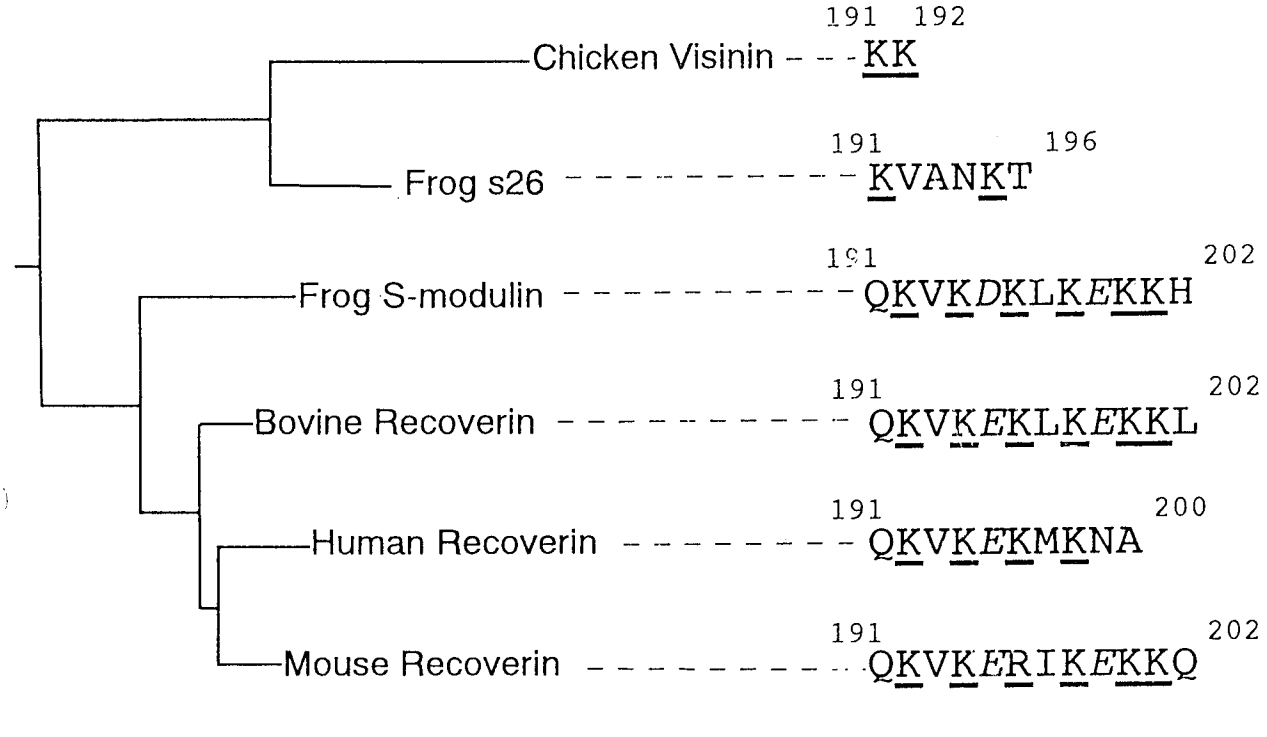

Figure 4-10: A Phylogenetic Tree (20) and C-terminal Amino Acid Sequences of Proteins in the S-modulin Family. Numbers represent amino acid numbers, counting from the N-terminus. Underlines and italic amino acids indicate the positively and negatively charged residues, respectively.

References

1. Stryer, L.(1986) Annu. Rev. Neurosci. 9, 87-119

2. Kaupp, U. B., and Koch, K.-W. (1992) Annu Rev. Physiol. 54, 153-175

3. Yau, K.-W., and Nakatani, K. (1985) Nature 313, 579-582

4. McNaughton, P. A., Cervetto, L., and Nunn, B. J. (1986) Nature 322, 261-263

5. Matthews, H. R., Murphy, R. L. W., Fain, G., and Lamb, T. D. (1988) Nature 334, 67-69

6. Nakatani, K., and Yau, K.-W. (1988) Nature 334, 69-71

7. Dizhoor, A.M., Ray, S., Kumar, S., Niemi, G., Spencer, M., Brolley, D., Walsh, K. A., Philipov, P. P., Hurley, J. B., and Stryer, L. (1991) Science 251, 915-918

8. Kawamura, S. (1993) Nature 362, 855-857

9. Kawamura, S., Hisatomi, O., Kayada, S., Tokunaga, F., and Kuo, C.-H. (1993) J. Bioi. Chem. 268, 14579-14582

10. Palczewski, K., Buczytko, J., Lebioda, L., Crabb, J. W., and Polans, A. S.(1993) J. Biol. Chem. 268, 6004-6013

11. Chen, J., Makino, C. L., Peachey, N. S., Baylor, D. A., and Simon, M. I.(1995) Science 267, 374-376

12. Zozulya, S., and Stryer, L. (1992) Proc. Natl. Acad. Sci. U.S.A. 89, 11569-11573

13. Dizhoor, A. M., Chen, C. K., Olshevskaya, E., Sinelnikova, V. V.,Phillipov, P., and Hurley, J. B. (1993) Science 259, 829-832

14. Haynes, L., and Yau, K.-W. (1985) Nature 317, 61-64

15. Cobbs, W. H., Barkdoll, A. E., and Pugh, E. N. (1985) Nature 317, 64-66

16. Nathans, J., Thomas, D., and Hogness, D. S. (1986) Science 232, 193-202

17. Lerea, C. L., Somers, D. E., Hurley, J. B., Klock, I. B., and Bunt-Milam, A. H. (1986) Science 234, 77-80

18. Hurwitz, R. L., Bunt-Milam, A. H., Chang, M. L., and Beavo, J. A. (1985) J. Biol. Chem. 260, 568-573

19. Baylor, D. A. (1987) Invest. Opthalmol. Visual Sci. 28, 34-49

20. Kawamura, S., Kuwata, O., Yamada, M., Matsuda, S., Hisatomi, O., and Tokunaga, F. (1996) J. Biol. Chem. 271, 21359-21364

21. Hisatomi, O., Ishino, T., Matsuda, S., Yamaguchi, K., Kobayashi, Y., Kawamura, S., and Tokunaga, F. (1997) Biochem. Biophys. Res. Commun. 234, 173-177

22. Kawamura, S., Cox, J. A., and Nef, P. (1994) Biochem. Biophys. Res. Commun. 203, 121-127

23. Sanada, K., Kokame, K., Yoshizawa, T., Takao, T., Shinonishi, Y. and Fukada, Y. (1995) J. Biol Chem. 270, 15459-15462

24. Kawamura, S., Takamatsu, K., and Kitamura, K. (1992) Biochem. Biophys. Res. Commun. 186, 411-417

25. Ames, J. B., Ishima, R., Tanaka, T., Gordon, J. I., Stryer, L., and Ikura, M (1997) Nature 389, 198-202

26. Flaherty, K. M., Zozolya, S., Stryer, L. and McKay, D. B. (1993) Cell 75, 709-716

27. Yamagata, K., Goto, K., Kuo, C.-H., Kondo, H., and Miki, N. (1990) Neuron 2, 469-476

28. Murakami, A., Yajima, T., and Inana, G. (1992)Biochem. Biophys. Res. Commun. 187, 234-244

29. McGinnis, J. F., Stepanik, P. L., Baehr, W., Subbaraya, I., and Lerious, V. (1992) FEBS Lett. 302, 172-176

30. Kraulis, P. J. (1991) J. Appl. Crystallogr 24, 946-950

Chapter 5

The Role of Calcium-binding sites on S-modulin Functions

Introduction

In vertebrate rod photoreceptors, cGMP-gated cation channels are opened in the dark-adapted state (1, 2). Light activates rhodopsin and triggers the phototransduction cascade, which results in the closure of the cation channels in the rod outer segment (ROS)1, and blocks the influx of Ca^{2+} . As intracellular Ca^{2+} is continuously pumped out by a Na^{+}-K^{+}/Ca^{2+} exchanger in the outer segment (3, 4). the cytoplasmic Ca^{2+} concentration decreases in the light-adapted photoreceptors. This decrease of Ca^{2+} concentration is the underlying mechanism of light adaptation of vertebrate photoreceptors (5, 6).

Phosphorylation of rhodopsin plays a role in shutting off the activation of transducin (7, 8), and the efficiency of phosphorylation is regulated, in a Ca^{2+}-dependent manner, by a Ca^{2+}-binding protein, frog S-modulin (9, 10) or its bovine homologue, recoverin (11). At high Ca^{2+} concentrations (dark-adapted state), S-modulin inhibits phosphorylation of light-activated rhodopsin, but does not interfere at low Ca^{2+} concentrations (light-adapted state). Therefore, S-modulin and recoverin contribute to increase light-sensitivity in the dark-adapted state.

These Ca^{2+}-binding proteins contain covalently attached fatty acyl groups at their N-terminus (12). The binding of Ca^{2+} to these proteins induces exposure of the fatty acyl groups, and enables them to associate with ROS membrane (13, 14). This property is the so-called "Ca^{2+}-myristoyl switch", and may be important for their function (13). There are four EF-hand motifs in S-modulin and recoverin, but only two of them (EF- 2 and 3) are thought to be able to bind Ca^{2+} (15). Therefore, S-modulin function (inhibition of rhodopsin phosphorylation) is mediated by the binding of Ca^{2+} ions to EF-2 and -3.

I made site-directed mutants of S-modulin that lack Ca^{2+}-binding ability of EF-2 or -3. The present paper describes the Ca^{2+}-binding properties, membrane-association and inhibitory effects on rhodopsin phosphorylation of wild-type S-modulin and these mutants. The results suggest that EF-3 first binds Ca^{2+}, which enables S-modulin to associate with ROS membrane and to accept Ca^{2+} at EF-2. This EF-2 binding of Ca^{2+} ions inhibits phosphorylation of rhodopsin.

Experimental Procedures

Site-directed mutagenesis—Site-directed mutants used in this study are shown in Figure 1. Oligonucleotides, 5'-GGTCATATGTAGCGCTATCATGTA CATCTTAAA-3' and 5'-TTGAATATTGCCGTAATGATTTCAAGCACCATTTTTTT-3' were used as anti-sense primers to generate site-directed mutants, E85M and E121M, respectively (Fig. 5-1). S-modulin cDNA fragment (10) and the SMD-NFT primer (16) were used as a template and sense primer for the polymerase chain reactions. cDNA fragments encoding E86M and E121M were inserted between NcoI and XhoI sites of pET-16b (Novagen) plasmid vector, designated pET-E85M and pET-E121M, respectively.

Expression and purification of recombinant proteins—The procedures for expression and purification of recombinants have been described by Hisatomi et al (16). Briefly, BL21DE3 (Novagen) previously transformed with pBB131 (an expression vector of *N*-myristoyl transferase; kindly provided by Prof. Jeffrey I. Gordon, Washington University) was co-transformed with pET-Smd (16), pET-E85M or pET-E121M, and the expression of myristoylated recombinants was induced by the addition of isopropyl-β-*D*-thiogalactopyranoside and myristic acid. Recombinant proteins were

solubilized in 8 M urea buffer, refolded by dialysis, and applied to a DEAE-Sephadex column. Further purification was carried out by using a phenyl-Sepharose column.

Ca^{2+}-Binding Assay— Binding of Ca^{2+} ions to S-modulin or mutant proteins was evaluated by ultra filtration (17) (shown in Fig. 5-2). Purified proteins were extensively dialyzed against 25 mM Tris-HCl (pH 8.0) to remove EGTA and calcium, then 20 μmol of each calcium free protein in 1 ml 25 mM Tris-HCl (pH 8.0) was placed on a Centricon-10 concentrator (Amicon). 1 ml 0.2 mM $CaCl_2$ solution in 25 mM Tris-HCl (pH 8.0) was then added and protein and calcium solution thoroughly mixed. The calcium-protein mixtures were centrifuged and the amounts of calcium in the filtrated fractions were measured by atomic absorption detector (Shimazu AA-660).

Tryptophan emission spectrum—Spectroscopic measurement was carried out as described by Hisatomi et al (16). Briefly, fluorescence emission spectra were recorded from 300 to 400 nm with a fluorescence spectrophotometer (Hitachi, F-4500) with an excitation wavelength at 290 nm, in mixture containing 2 μM recombinant protein, 100 mM KCl, 5 mM 2-mercaptoethanol and 1 mM EGTA, 100 mM HEPES (pH 7.0). Free Ca2+ concentration was adjusted by adding 1 M $CaCl_2$.

Ca^{2+}-dependent membrane association of recombinant proteins — Membrane association of wild type and mutant S-modulins were investigated as shown in Figure 5-4. Frog ROS were isolated by flotation with 45% sucrose in gluconate buffer (40mM K-gluconate, 2.5 mM KCl, 2 mM $MgCl_2$, 1 mM DTT, 1 mM EGTA 10 mM HEPES, pH 7.5), and washed with gluconate buffer containing 4 M urea to eliminate endogenous S-modulin and s26 (cone homologue of S-modulin), and other peripheral proteins. Urea-stripped ROS membranes were mixed with gluconate buffer containing 1%

bovine serum albumin to prevent non-specific binding of the recombinant proteins to the ROS membrane and tube. After washing with gluconate buffer containing various concentrations of Ca^{2+} (Ca^{2+} gluconate buffer), the ROS membranes were re-suspended in Ca^{2+} gluconate buffer containing recombinant proteins (120 pmol). The mixtures were incubated at room temperature for 30 min, and the soluble and membrane fractions after centrifugation (37,000 x g for 5 min) were analyzed by SDS-PAGE. The integrated densities of Coomassie Brilliant Blue (CBB) stained bands of the recombinant proteins were quantified by a two dimensional densitometer (pdi. The Discovery Series).

Phosphorylation assay—Phosphorylation of rhodopsin was measured by the method described by Kawamura (9) and Sanada et al (18) (shown in chapter 4). For the phosphorylation assay, ROS were isolated in phosphorylation buffer (115 mM K-gluconate, 2.5 mM KCl, 2 mM $MgCl_2$, 1 mM DTT, 1 mM EGTA, 10 mM HEPES, pH 7.5) in complete darkness, and washed with the buffer to eliminate endogenous S-modulin, s26 and ATP. The reaction was carried out in 25μl of the mixture, containing 10 μM (final concentration) of rhodopsin and 5 μM of S-modulin or its mutants in phosphorylation buffer. Free calcium concentration in the mixture was adjusted by adding 1M $CaCl_2$ solution. The reaction mixtures were exposed to light for 2 min, and the reaction was initiated by addition of a mixture of ATP (0.1 mM final concentration), [γ-^{32}P] ATP (168 TBq/μmol, 0.25 μM) and GTP (0.5 mM). After 2 min incubation at room temperature, the reaction was terminated by adding 150 μl 10% trichloroacetic acid. After centrifugation (10,000 x g for 5 min) of the reaction mixture, the precipitates were washed with 500 μl of phosphorylation buffer and applied to SDS-PAGE. The amount of ^{32}P incorporated into rhodopsin was quantified by using an image analyzer (BAS 2000, Fuji Film).

Results and Discussions

Ca^{2+}-binding of S-modulin and mutants—It has been established that the conserved glutamic acid at position 12 of the Ca^{2+}-binding loop is important for coordinating Ca^{2+} (19, 20). To investigate the role of each Ca^{2+}-binding site, EF-2 or EF-3 was inactivated by replacing glutamic acid with the hydrophobic amino acid, methionine. Myristoylated wild-type and mutant (E85M and E121M) S-modulins were expressed and purified as described in the experimental procedures. The number of Ca^{2+} ions bound to each of these proteins was quantified in the presence of 0.1 mM Ca^{2+} (Table 5-1). As expected, wild-type S-modulin and E85M bind two and one Ca^{2+} per a molecule, respectively. On the other hand, E121M can not bind Ca^{2+}. These results indicate that Ca^{2+}-binding to EF-3 is necessary for EF-2 to bind Ca^{2+} at physiological Ca^{2+} concentrations. It has been reported that EF-3 has the conformation of a classic EF-hand, but EF-2 is rather different (21). The conformational change induced by Ca^{2+}-binding to EF-3 may be required for EF-2 to be a functional EF-hand.

Fluorescence properties of S-modulin and mutants—E85M and E121M can be purified as wild-type S-modulin, so it seems that the structure of S-modulin is not largely disrupted by the mutagenesis. Figure 5-3 shows the tryptophan emission spectra of the wild type and mutant S-modulins. Wild-type S-modulin, E85M and E121M showed almost the same spectrum in the presence of 1 nM Ca^{2+} (Fig. 5-3 upper panel). This suggests that the mutations of glutamic acid to methionine in EF-2 or EF-3 do not significantly change the environment of the three tryptophan residues in the Ca^{2+}-free form of these proteins. However, the emission spectra of mutants were different from that of wild-type at 0.1 mM Ca^{2+} concentration (Fig. 5-3 lower panel): The

spectrum of the wild-type is red-shifted by increasing Ca^{2+} concentration (16); that of E85M shows a smaller red-shift; and that of E121M was not affected by Ca^{2+} concentration. The red-shift observed in E85M, which can bind one Ca^{2+} ion per a molecule, is probably caused by the binding of Ca^{2+} to EF-3.

Membrane association of wild-type, E85M and E121M S-modulins — The recombinant S-modulin (wild-type or E85M or E121M) was mixed with urea-stripped ROS membranes at various Ca^{2+} concentrations, and separated by centrifugation into membrane and soluble fractions. The soluble fraction (containing proteins free from ROS membrane) and the membrane fractions (containing proteins bound to ROS membrane) were subjected to SDS-PAGE. The densities of CBB stained bands of the wild-type and mutant S-modulins were analyzed quantitatively, and the ratio of membrane bound protein, (membrane fraction)/(membrane + soluble fraction), was plotted against Ca^{2+} concentration (Fig. 5-5). This shows that E85M has almost the same membrane affinity as the wild-type, suggesting that binding of Ca^{2+} to EF-3 induces exposure of the myristoyl group. It is reported that the ejection of myristoyl group is required for the rotation at Gly 42, the unclamping of the myristoyl group and the melting of part of the N-terminal helix (21). Ca^{2+}-binding to EF-3 may induce these changes until the level necessary for membrane association.

As E121M can not bind Ca^{2+} at concentrations less than 0.1 mM Ca^{2+} , it can hardly bind to the ROS membrane at all, although in the presence of 1mM Ca^{2+}, E121M does bind slightly. This may be explained by the binding of Ca^{2+} to EF-2 or inactivated EF-3 at very high (more than 1mM) Ca^{2+} concentration, which is well above normal physiological Ca^{2+} concentrations.

Inhibition of rhodopsin phosphorylation by wild-type or mutant S-modulins—Figure 5-6 shows the incorporation of ^{32}P-labeled phosphatic acid into rhodopsin in the presence of wild-type or E85M or E121M S-modulins. Wild-type S-modulin inhibits rhodopsin phosphorylation at high (0.1 mM) Ca^{2+} concentration, but neither E85M nor E121M can inhibit rhodopsin phosphorylation even at high Ca^{2+} concentration. This indicates that the Ca^{2+} binding to EF-3 is not enough to inhibit rhodopsin phosphorylation, and suggests that Ca^{2+} binding to EF-2 is important for the inhibitory activity of S-modulin.

A model for Ca^{2+}-binding and conformational changes of S-modulin —I propose a model to explain the Ca^{2+}-binding properties and induced conformational changes of S-modulin (Fig. 5-7). In the Ca^{2+} free state (upper panel), EF-3 is thought to be the only functional Ca^{2+}-binding site. If there is enough Ca^{2+}, EF-3 binds Ca^{2+} (middle panel), which causing exposure of the myristoyl group which converts EF-2 to a functional Ca^{2+}-binding site. If the Ca^{2+} affinity of resulting EF-2 is high, cooperative Ca^{2+} binding (22) can be explained. Finally, EF-2 binds Ca^{2+} and S-modulin can now inhibit rhodopsin phosphorylation (lower panel).

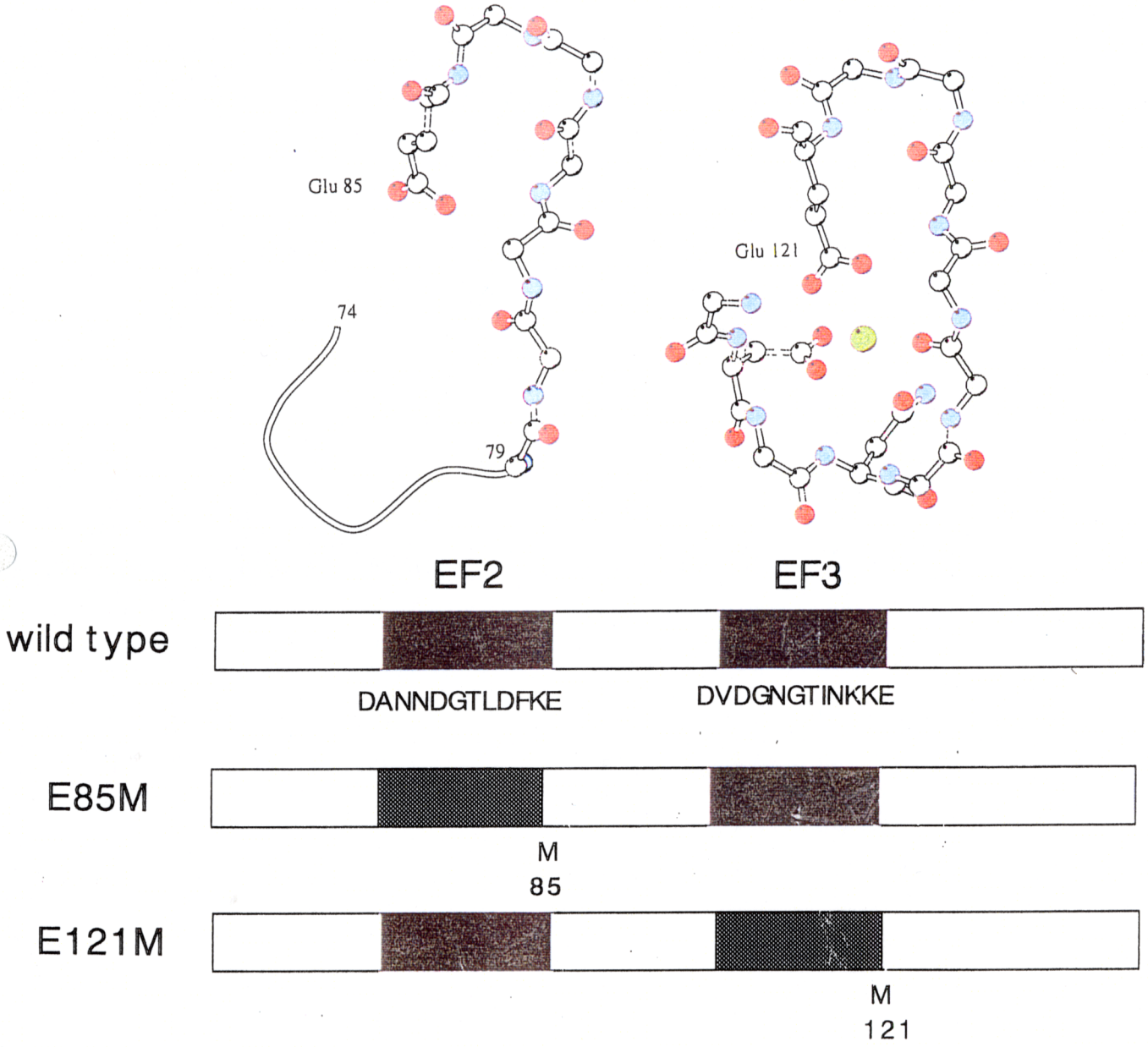

Figure 5-1: Ball and stick models of the roops of the two functional EF-hands of bovine S-modulin (oxygens are red; nitrogens, blue; calcium bound to EF3, green), and site-directed mutants used in this study

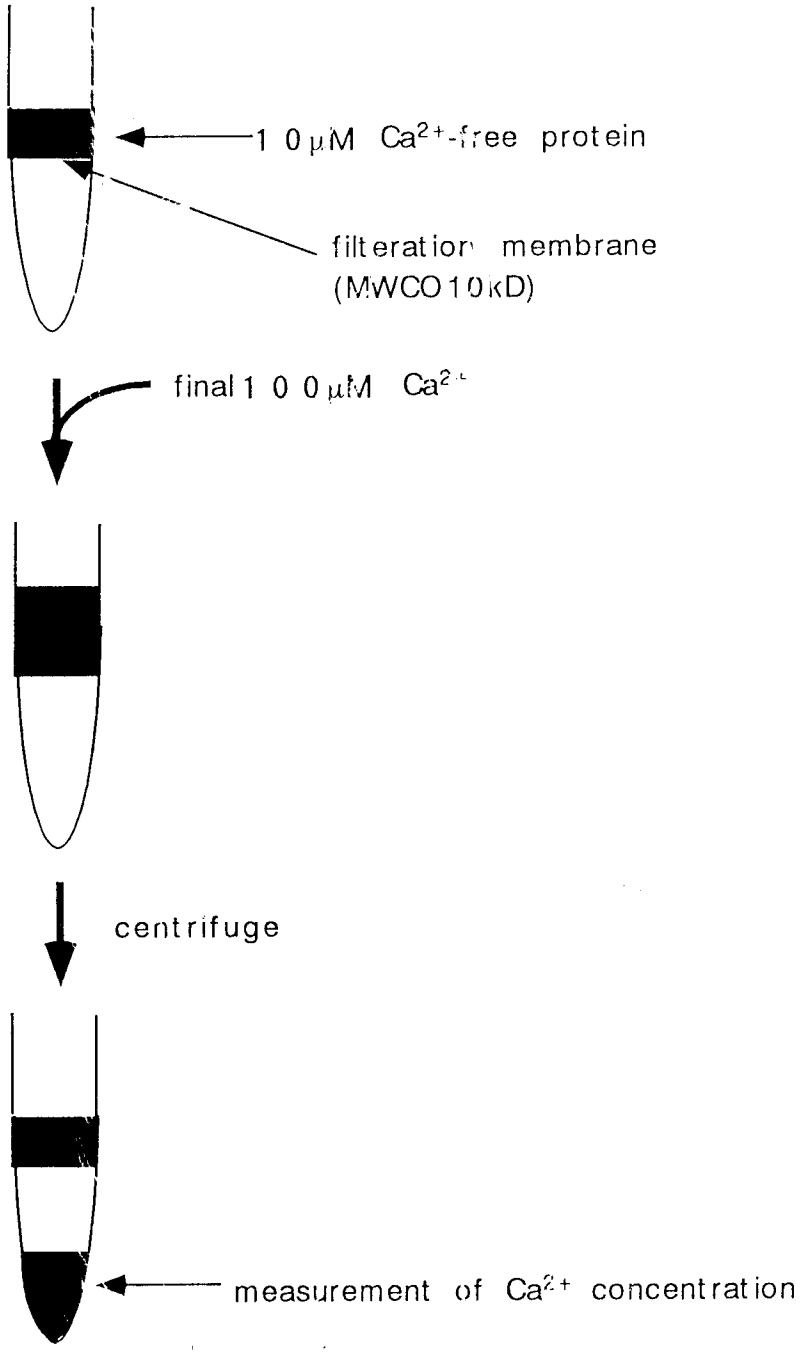

Figure 5-2: A method of ultra filtration

	No. of Calcium ions bound
wild-type	2.1±0.10
E85M	0.97±0.02
E121M	0.02±0.04

Table 5-1: The number of Ca^{2+} ions bound to wild-type, E85M and E121M S-modulin (per molecule) in the presence of 0.1 mM Ca^{2+}.

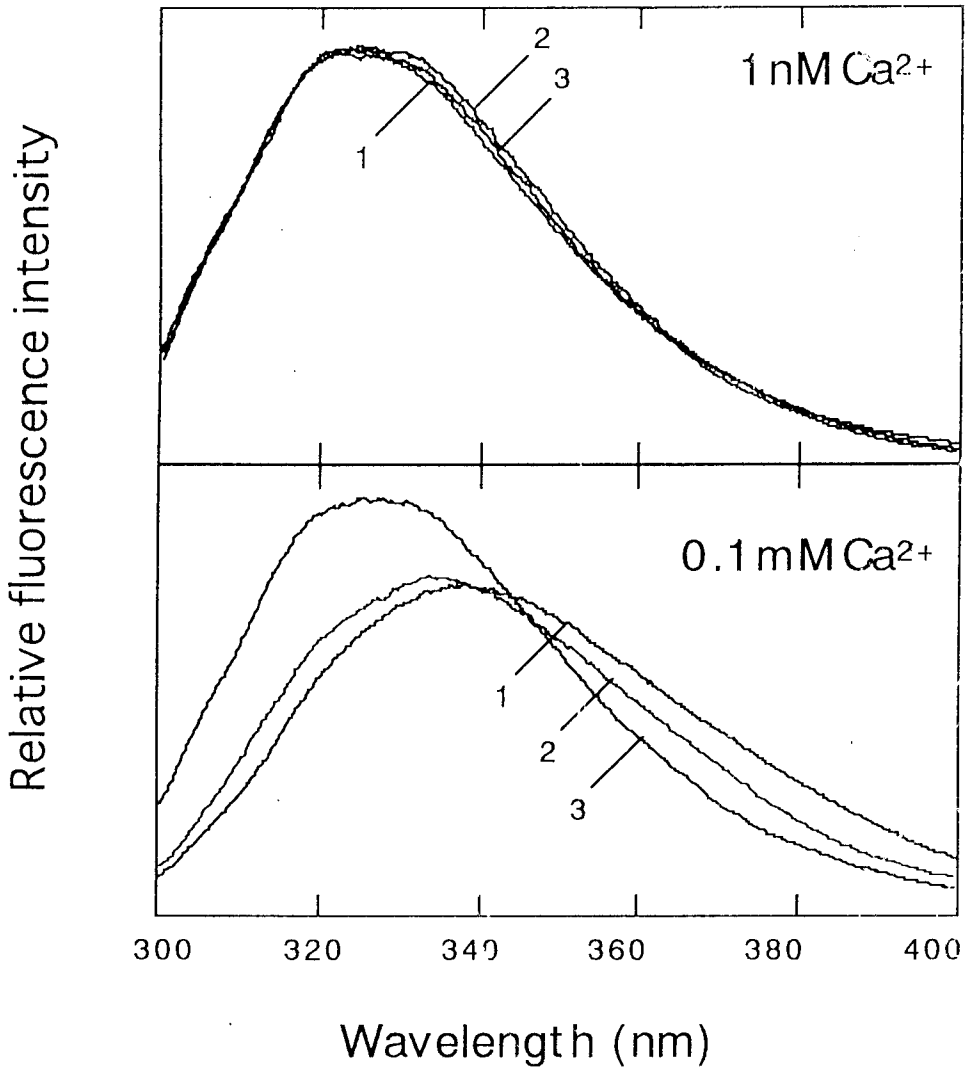

Figure 5-3: Tryptophan emission spectra of wild-type and mutant S-modulins. Fluorescence emission spectra of wild-type S-modulin (curve 1), E85M (curve 2) and E121M (curve 3) in the presence of 1 nM (upper panel) and 0.1 mM (lower panel) free Ca^{2+}.

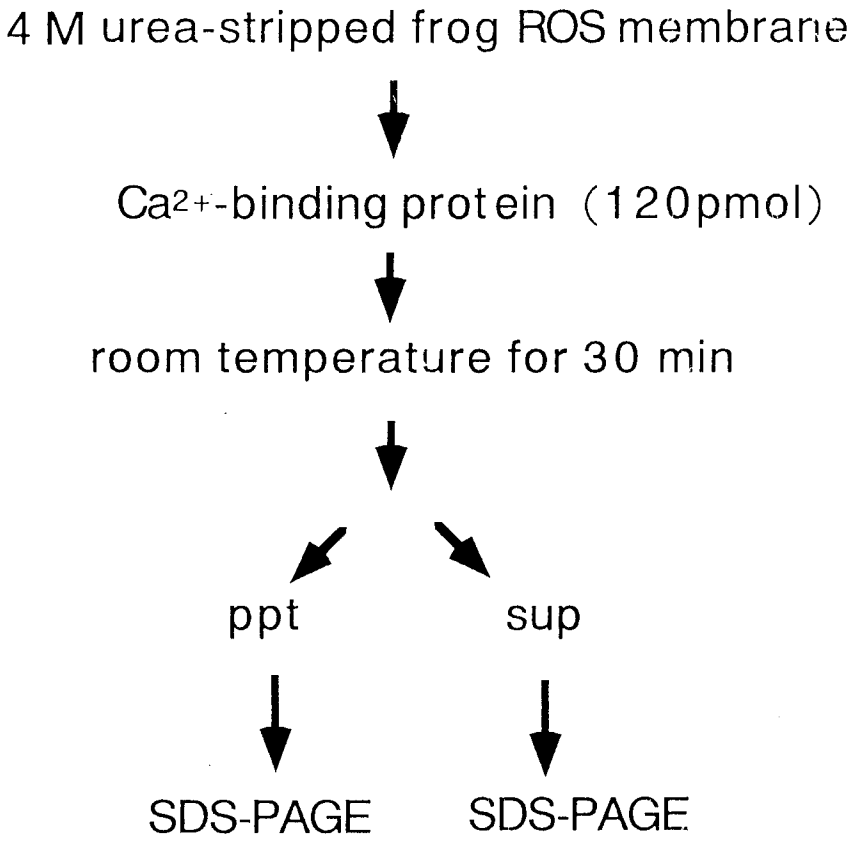

Figure 5-4: A method to investigate membrane-binding properties of recombinant proteins

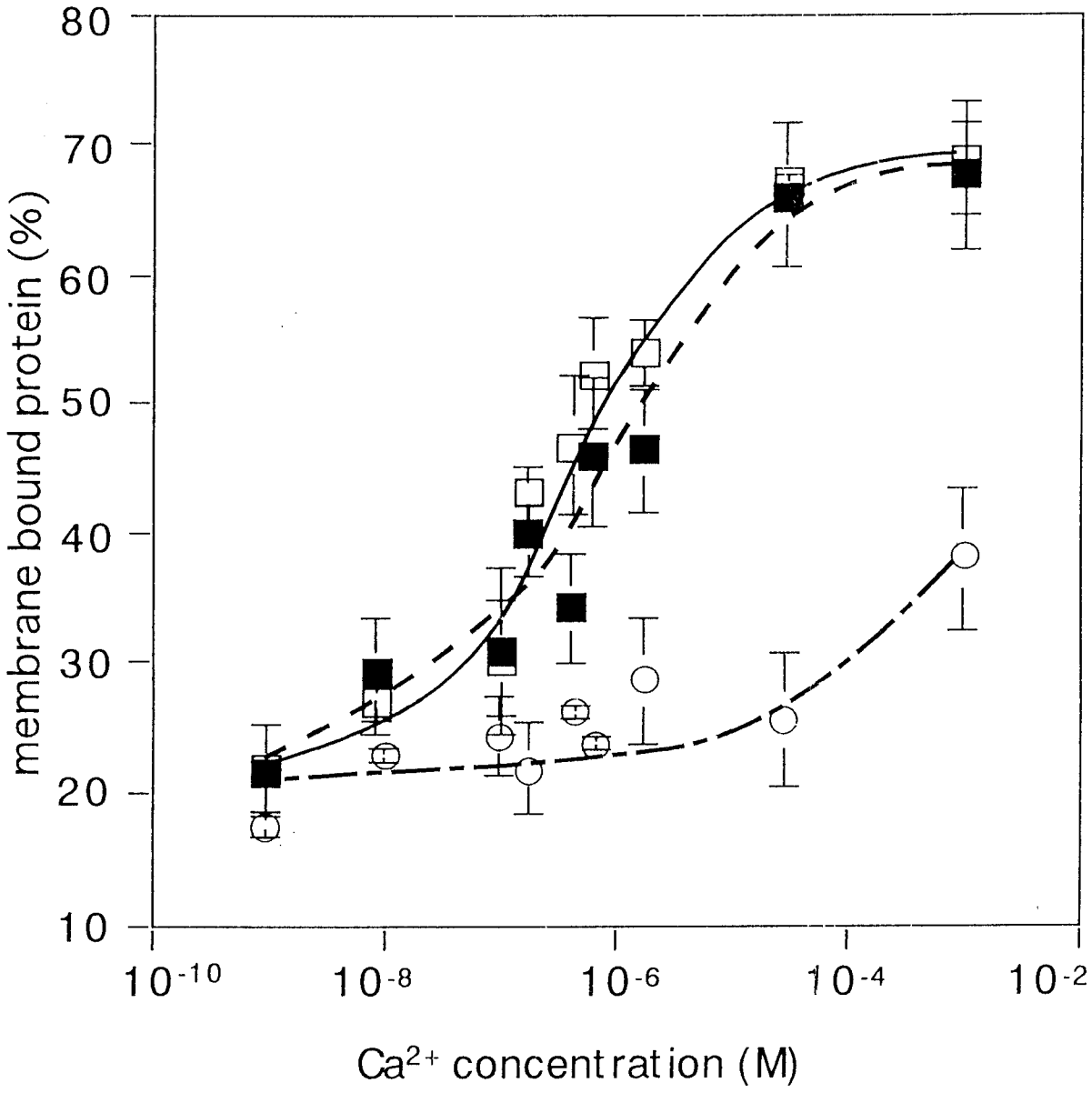

Figure 5-5: Membrane-binding properties of wild-type and mutant S-modulins. The ROS membrane affinity of wild-type, E85M and E121M at various Ca^{2+} concentrations. Bars represent standard deviations (n = 2). □: wild-type S-modulin, ■: E85M, ○: E121M.

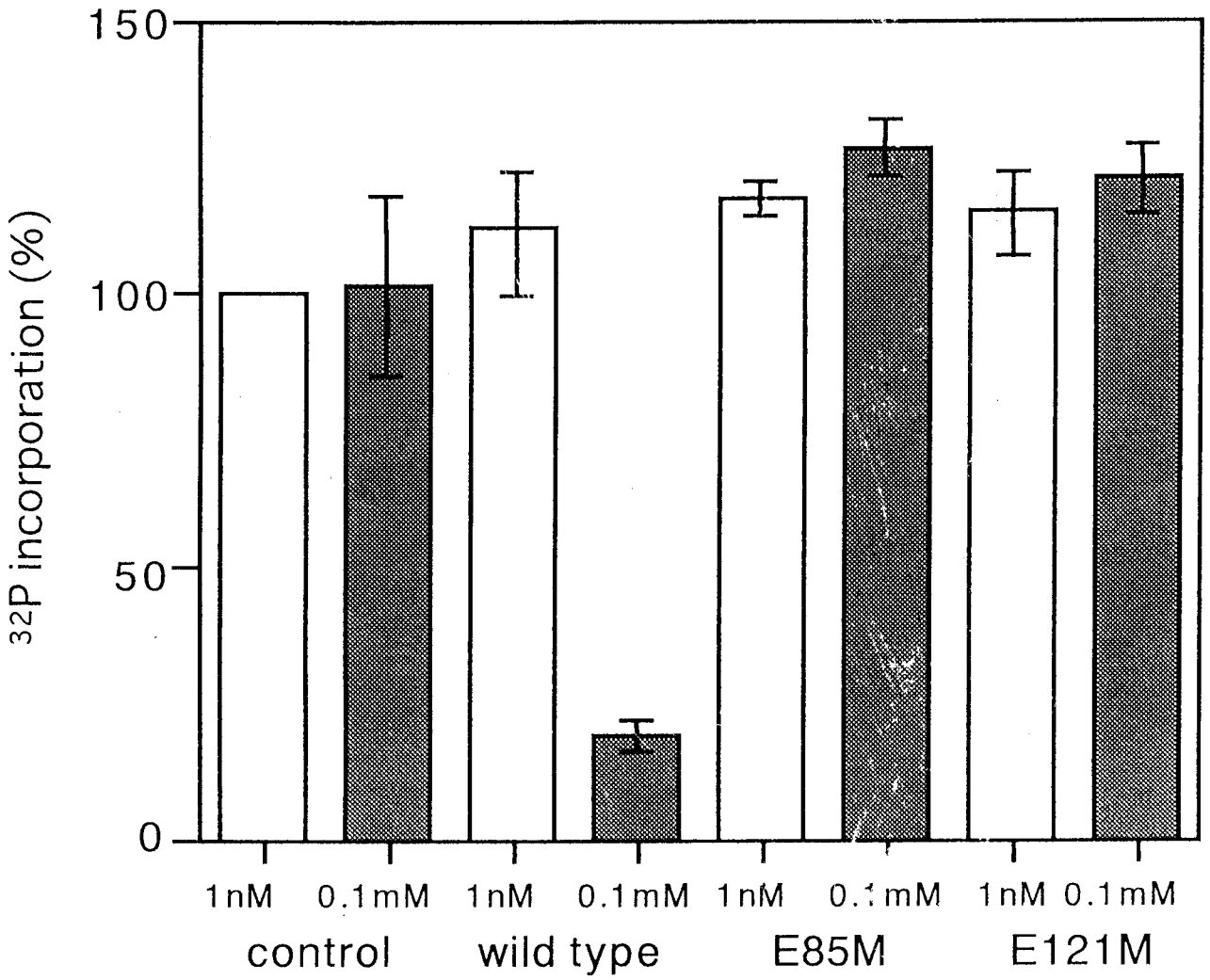

Figure 5-6: Inhibition of rhodopsin phosphorylation by wild-type and mutant S-modulins. ^{32}P-incorporation of rhodopsin in the presence of [γ-^{32}P] ATP at low (1 nM; open bars) and high (0.1 mM; shaded bars) Ca^{2+} concentration. Experiments were carried out without recombinant protein (control) or in the presence of 5 μM S-modulins (wild-type, E85M or E121M). Bars represent standard deviations (n = 2).

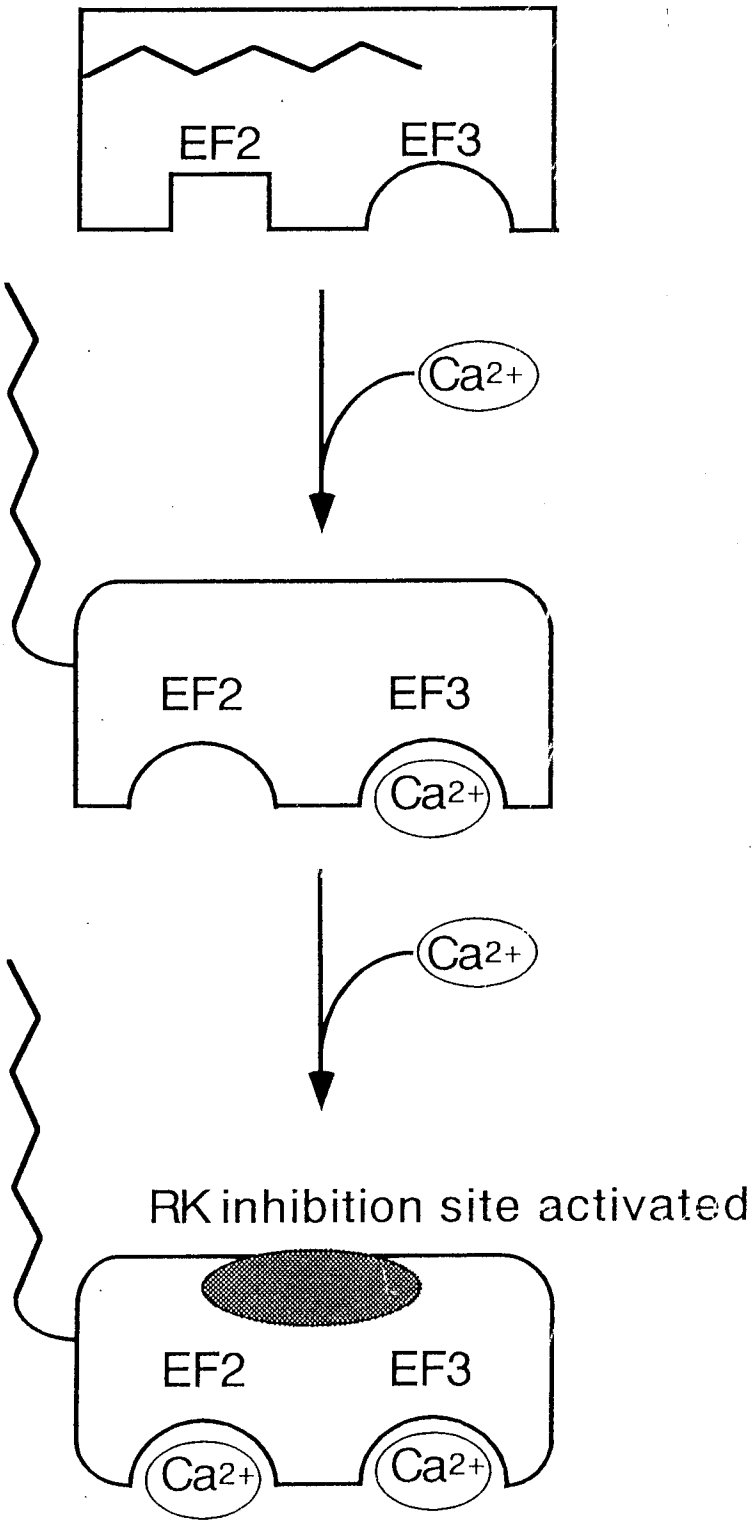

Figure 5-7: A model for Ca^{2+} induced structural changes of S-modulin.

References

1. Stryer, L.(1986) Annu. Rev. Neurosci. 9, 87-119

2. Kaupp, U. B., and Koch, K.-W. (1992) Annu Rev. Physiol. 54, 153-175

3. Yau, K.-W., and Nakatani, K. (1985) Nature 313, 579-582

4. McNaughton, P. A., Cervetto, L., and Nunn, B. J. (1986) Nature 322, 261-263

5. Matthews, H. R., Murphy, R. L. W., Fain, G., and Lamb, T. D. (1988) Nature 334, 67-69

6. Nakatani, K., and Yau, K.-W. (1988) Nature 334, 69-71

7. Palczewski, K., Buczytko, J., Lebioda, L., Crabb, J. W., and Polans, A. S.(1993) J. Biol. Chem. 268, 6004-6013

8. Chen, J., Makino, C. L., Peachey, N. S., Baylor, D. A., and Simon, M. I.(1995) Science 267, 374-376

9. Kawamura, S. (1993) Nature 362, 855-857

10. Kawamura, S., Hisatomi, O., Kayada, S., Tokunaga, F., and Kuo, C.-H. (1993) J. Bioi. Chem. 268, 14579-14582

11. Dizhoor, A.M., Ray, S., Kumar, S., Niemi, G., Spencer, M., Brolley, D., Walsh, K. A., Philipov, P. P., Hurley, J. B., and Stryer, L. (1991) Science 251, 915-918

12. Dizhoor, A. M., Ericsson, L. H., Johnson, R. S., Kumar, S., Olshevskaya, E., Zozulya, S., Neubert, T. A., Stryer, L., Hurley, J. B., and Walsh, K. A. (1992) J. Biol. Chem. 267, 16033-16036

13. Zozulya, S., and Stryer, L. (1992) Proc. Natl. Acad. Sci. U.S.A. 89, 11569-11573

14. Dizhoor, A. M., Chen, C. K., Olshevskaya, E., Sinelnikova, V. V.,Phillipov, P., and Hurley, J. B. (1993) Science 259, 829-832

15. Flaherty, K. M., Zozulya, S., Stryer, L. and Mckay, D. B. (1993) Cell 75, 709-716

16. Hisatomi, O., Ishino, T., Matsuda, S., Yamaguchi, K., Kobayashi, Y., Kawamura, S., and Tokunaga, F. (1997) Biochem. Biophys. Res. Commun. 234, 173-177

17. Blatt, W. F. and Robinson, S. M. (1968) Analytical Biochemistry 26, 151-173

18. Sanada, K., Kokame, K., Yoshizawa, T., Takao, T., Shinonishi, Y. and Fukada, Y. J. Biol Chem. (1995) 270, 15459-15462

19. Strynadka, C. J. and James M. N. G. (1989) Annu. Rev. Biochem. 58, 951-998

20. Babu, A., Su, H., Ryu, Y. and Glati, J. (1992) J. Biol Chem. 267, 15469-15474

21. Ames, J. B., Ishima, R., Tanaka, T., Gordon, J. I. Stryer, L. and Ikura, M. (1997) Nature 389, 198-202

22. Ames, J. B., Porumb, T., Tanaka, T., Ikura, M., and Stryer, L (1995) J. Biol. Chem. 270, 4526-4533

Acknowledgments

I thank Prof. Fumio Tokunaga, Prof. Satoru Kawamura, Prof. Yuji Kobayashi, Dr. Osamu Hisatomi, Dr. Ian G. Greadal, Mr. Tetsuya Ishino, and Ms. Kumiko Nanda for their continuous supports and helpful discussions. I thank Prof. Mikio Kataoka, Dr. Kouichi Ozaki, Dr. Yasushi Imamoto for their helpful suggestion. I thank Prof. Jeffrey I. Gordon for kind gift of an expression vector of *N*-myristoyl transferase. I also thank Prof. Takashi Kurahashi for comments on the manuscript. The works written in Capter 2 and 3 are joint researches with several people: I thank Prof. Kawamura for doing immunohistochemistry in Chapter 2, and phosphorylation experiments in Chapter 3; I also thank Prof. Kobayashi and Mr. Ishino for doing CD spectra measurements. This work was supported in part by JSPS Fellowships for Young Scientists, by a Grant-in-Aid for Scientific Research from Japanese Ministry of Education, Culture and Science and by SUNBOR.